

University of Nebraska - Lincoln

DigitalCommons@University of Nebraska - Lincoln

United States Department of Agriculture Wildlife
Services: Staff Publications

U.S. Department of Agriculture: Animal and
Plant Health Inspection Service

2024

Reemergence of a Big Brown Bat *Lyssavirus rabies* Variant in Striped Skunks in Flagstaff, Arizona, USA, 2021–2023

Amy T. Gilbert

United States Department of Agriculture, Animal and Plant Health Inspection Service, Wildlife Services, National Wildlife Research Center, Fort Collins, Colorado, amy.t.gilbert@usda.gov

Lolita I. Van Pelt


United States Department of Agriculture, Animal and Plant Health Inspection Service, Wildlife Services, Phoenix, Arizona, lolita.i.vanpelt@usda.gov

Lias A. Hastings

United States Department of Agriculture, Animal and Plant Health Inspection Service, Wildlife Services, Phoenix, Arizona, Lias.Hastings@usda.gov

Follow this and additional works at: https://digitalcommons.unl.edu/icwdm_usdanwrc

Crystal M. Gigante

 *Center for Disease Control and Prevention, National Center for Emerging and Zoonotic Infectious Diseases, Rabies and Raccoon Branch*

Public Health Sciences Commons, Other Environmental Sciences Commons, Other Veterinary Medicine Commons, Population Biology Commons, Terrestrial and Aquatic Ecology Commons, Veterinary Infectious Diseases

Lillian A. Orciari

Center for Disease Control and Prevention, National Center for Emerging and Zoonotic Infectious Diseases, Rabies and Raccoon Branch

Epidemiology, and Public Health Commons, and the Zoology Commons

~~Gilbert, Amy T.; Van Pelt, Lolita I.; Hastings, Lias A.; Gigante, Crystal M.; Orciari, Lillian A.; Kelley, Sabrina; Fitzpatrick, Kathryn; Condori, René Edgar; Li, Yu; Brunt, Scott; Davis, April; Hopken, Matthew W.; Mankowski, Clara C. P.; Wallace, Ryan M.; Rupprecht, Charles E.; Chipman, Richard B.; and Bergman, David L., "Reemergence of a Big Brown Bat *Lyssavirus rabies* Variant in Striped Skunks in Flagstaff, Arizona, USA, 2021–2023" (2024). *United States Department of Agriculture Wildlife Services: Staff Publications*. 2823.~~

https://digitalcommons.unl.edu/icwdm_usdanwrc/2823

This Article is brought to you for free and open access by the U.S. Department of Agriculture: Animal and Plant Health Inspection Service at DigitalCommons@University of Nebraska - Lincoln. It has been accepted for inclusion in United States Department of Agriculture Wildlife Services: Staff Publications by an authorized administrator of DigitalCommons@University of Nebraska - Lincoln.

Authors

Amy T. Gilbert, Lolita I. Van Pelt, Lias A. Hastings, Crystal M. Gigante, Lillian A. Orciari, Sabrina Kelley, Kathryn Fitzpatrick, René Edgar Condori, Yu Li, Scott Brunt, April Davis, Matthew W. Hopken, Clara C. P. Mankowski, Ryan M. Wallace, Charles E. Rupprecht, Richard B. Chipman, and David L. Bergman

Open camera or QR reader and
scan code to access this article
and other resources online.



Reemergence of a Big Brown Bat *Lyssavirus rabies* Variant in Striped Skunks in Flagstaff, Arizona, USA, 2021–2023

Amy T. Gilbert,¹ Lolita I. Van Pelt,² Lias A. Hastings,² Crystal M. Gigante,³ Lillian A. Orciari,³ Sabrina Kelley,⁴ Kathryn Fitzpatrick,⁵ Rene E. Condori Condori,³ Yu Li,³ Scott Brunt,⁶ April Davis,⁶ Matthew W. Hopken,¹ Clara C. P. Mankowski,¹ Ryan M. Wallace,³ Charles E. Rupprecht,⁷ Richard B. Chipman,⁸ and David L. Bergman²

Abstract

Background: Throughout the Americas, *Lyssavirus rabies* (RV) perpetuates as multiple variants among bat and mesocarnivore species. Interspecific RV spillover occurs on occasion, but clusters and viral host shifts are rare. The spillover and host shift of a big brown bat (*Eptesicus fuscus*) RV variant Ef-W1 into mesocarnivores was reported previously on several occasions during 2001–2009 in Flagstaff, Arizona, USA, and controlled through rabies vaccination of target wildlife. During autumn 2021, a new cluster of Ef-W1 RV cases infecting striped skunks (*Mephitis mephitis*) was detected from United States Department of Agriculture enhanced rabies surveillance in Flagstaff. The number of Ef-W1 RV spillover cases within a short timeframe suggested the potential for transmission between skunks and an emerging host shift.

Materials and Methods: Whole and partial RV genomic sequencing was performed to evaluate the phylogenetic relationships of the 2021–2023 Ef-W1 cases infecting striped skunks with earlier outbreaks. Additionally, real-time reverse-transcriptase PCR (rtRT-PCR) was used to opportunistically compare viral RNA loads in brain and salivary gland tissues of naturally infected skunks.

Results: Genomic RV sequencing revealed that the origin of the 2021–2023 epizootic of Ef-W1 RV was distinct from the multiple outbreaks detected from 2001–2009. Naturally infected skunks with the Ef-W1 RV showed greater viral RNA loads in the brain, but equivalent viral RNA loads in the mandibular salivary glands, compared to an opportunistic sample of skunks naturally infected with a South-Central skunk RV from northern Colorado, USA.

Conclusion: Considering a high risk for onward transmission and spread of the Ef-W1 RV in Flagstaff, public outreach, enhanced rabies surveillance, and control efforts, focused on education, sample characterization, and vaccination, have been ongoing since 2021 to mitigate and prevent the spread and establishment of Ef-W1 RV in mesocarnivores.

Keywords: host shift, *Lyssavirus rabies*, spillover, surveillance, wildlife, zoonosis

¹United States Department of Agriculture, Animal and Plant Health Inspection Service, Wildlife Services, National Wildlife Research Center, Fort Collins, Colorado, USA.

²United States Department of Agriculture, Animal and Plant Health Inspection Service, Wildlife Services, Phoenix, Arizona, USA.

³National Center for Emerging and Zoonotic Infectious Diseases, Poxvirus and Rabies Branch, Centers for Disease Control and Prevention, Atlanta, Georgia, USA.

⁴Coconino County Health and Human Services, Flagstaff, Arizona, USA.

⁵Arizona Department of Health Services, Phoenix, Arizona, USA.

⁶New York State Department of Health, Wadsworth Center Rabies Laboratory, Slingerlands, New York, USA.

⁷Auburn University, College of Forestry, Wildlife, and the Environment, Auburn, Alabama, USA.

⁸United States Department of Agriculture, Animal and Plant Health Inspection Service, Wildlife Services, National Rabies Management Program, Concord, New Hampshire, USA.

Introduction

The process of viral emergence in a novel host involves multiple stages, but at minimum requires a productive spillover infection in the novel host and contact between the reservoir host and novel host or population (Childs et al 2007; Plowright et al 2017). Later stages of the process, which may be nonessential for emergence but serve as evidence of a host shift, include sustained viral transmission within the novel host in the absence of new spillover infections and potential viral adaptation to the novel host (Childs et al 2007; Plowright et al 2017). Ecological requirements for the emergence of zoonoses are often met through overlapping geographic distribution and spatial activity of reservoirs and novel hosts, whereas taxonomic diversity and relatedness are also strong modifying evolutionary factors impacting viral zoonotic risk (Mollentze and Streicker, 2020; Jacquot et al, 2022).

The history of *Lyssavirus rabies* (RV) evolution has repeatedly involved spillover and host shifts (Badrane and Tordo, 2001; Troupin et al, 2016). All mammals are susceptible to RV infection, in part because RV infects the nervous system via conserved receptor-binding domains, e.g., the nicotinic acetylcholine receptor (Jackson, 2020). Empirical studies of suspected wildlife RV host shift events have reported that selection upon the RV genome in a new host is transient and may not follow consistent nor predictable pathways of adaptation, with potential preadaptation of some RV variants to spillover (Kuzmin et al, 2012; Streicker et al, 2012; Borucki et al, 2013; Marston et al, 2017; Streicker and Biek, 2020). Throughout the Americas, RV is enzootic in multiple bat and mesocarnivore reservoir species (Gilbert, 2018), where transmission mostly occurs among conspecifics (Carey and McLean, 1983; Smith, 1989). It remains unclear why most RV variants are maintained by a single species reservoir in the Americas (Rupprecht et al, 2011). A mechanistic understanding of the host factors influencing this phenomenon has been lacking, yet a recent review synthesized hundreds of empirical studies and concluded that the relatedness between hosts may constrain RV pathobiology and can influence viral evolutionary adaptation and onward transmission in novel populations or species (Fisher et al, 2018; Mollentze et al, 2020).

Spillovers and host shifts of bat RV have been documented previously (Streicker et al, 2010; Streicker et al, 2012), yet the detection of spatiotemporal clusters of bat RV spillover in mesocarnivores has been rarely reported (Daoust et al, 1996). Unique evidence of multiple independent bat RV spillover events and host shifts into striped skunks (*Mephitis mephitis*) and gray foxes (*Urocyon cinereoargenteus*) in Flagstaff, Arizona, USA, was described during 2001–2009, associated with the big brown bat (*Eptesicus fuscus*) RV variant Ef-W1 (Leslie et al, 2006; Blanton et al, 2010; Kuzmin et al, 2012). While distinct outbreaks of Ef-W1 RV in mesocarnivores were reported during 2001, 2004–2005 and 2008–2009 in Arizona, only the 2001 and 2008–2009 cases formed independent monophyletic clusters (Kuzmin et al, 2012). Collaborative responses to the 2001–2009 outbreaks in Flagstaff, Arizona, were led jointly by Coconino County and the United States Department of Agriculture (USDA) involving enhanced rabies surveillance (ERS) and targeted wildlife rabies management to protect human and animal health (Slate et al, 2009).

On August 5, 2021, an RV spillover was confirmed in a striped skunk by the Wildlife Services program of the USDA,

Animal and Plant Health Inspection Service (APHIS), in Phoenix, Arizona, USA. By December 31, 2021, 16 striped skunks were confirmed to be infected with Ef-W1 RV. We characterize the Ef-W1 RV infecting striped skunks during 2021–2023 in northern Arizona, USA, and compare it to prior outbreaks in the area using partial- and whole-genome sequencing (WGS). We also examined and compared the RV RNA loads in brains and salivary glands of naturally infected skunks, as a proxy of the potential for shedding, transmission, and spread of Ef-W1 RV in striped skunk populations of northern Arizona, USA.

Methods and Materials

Wildlife reported by the public or private organizations were submitted for RV diagnosis as part of ERS, by the USDA APHIS Wildlife Services and using the direct rapid immunohistochemical test (Patrick et al, 2019; Rupprecht et al, 2022), or for rabies public health surveillance by the Arizona Department of Health Services, Bureau of State Laboratory Services, Phoenix, Arizona, USA, using the direct fluorescent antibody test (Ronald et al, 2003). Brain samples from rabid animals were sent for typing and genomic characterization at either the Centers for Disease Control and Prevention (CDC), Poxvirus and Rabies Laboratory or the Wadsworth Rabies Laboratory of the New York State Department of Health. Carcasses from 15 rabid and two RV-negative striped skunks were shipped to the USDA APHIS Wildlife Services National Wildlife Research Center, Fort Collins, Colorado, USA, for postmortem tissue collection and real-time reverse-transcriptase polymerase chain reaction (rtRT-PCR) assay of brain and salivary gland tissues.

We opportunistically included parallel data and rtRT-PCR results from a pre-existing collaboration and archive of post-mortem samples, comprised of 32 confirmed rabid striped skunks and seven RV-negative skunks that had been submitted for public health surveillance to the Colorado State University Veterinary Diagnostic Laboratory during 2018–2019. Sample RNA isolation methods are provided in the Supplementary Data S1.

Lyssavirus Rabies Typing and Genomic Sequencing

At Wadsworth laboratory, RV typing was performed using a modified triplex rtRT-PCR assay, amplifying two separate regions of the RV nucleoprotein (Nadin-Davis et al, 2009) and a beta-actin mRNA internal positive control (IPC; Wadhwa et al, 2017) on the Applied Biosystem 7500 FAST platform (Thermo Fisher Scientific, Waltham, MA, USA).

At the CDC laboratory, complete RV nucleoprotein and glycoprotein gene sequencing was performed as described in Dettinger et al (2022), except that RT and primary PCR was performed using SuperScript IV one-step reverse transcriptase-PCR system (Thermo Fisher, Waltham, MA, USA) following the manufacturer's recommendations in 20 μ L reactions. Sequencing was performed on the MinION using a flongle flow cell version FLG001 after library preparation with the LSK-109 ligation sequencing kit and EXP-PBC096 PCR barcoding kit (Oxford Nanopore Technologies, Oxford, UK). Basecalling was performed using guppy version 4.2.2 (Oxford Nanopore Technologies, Oxford, UK). Reference-based consensus sequences were generated using ivar 0.1 (<https://github.com/andersen-lab/ivar>) from mapping output of minimap2 v.2.16

(<https://github.com/lh3/minimap2>) and polished using medaka v1.0.1 (<https://github.com/nanoporetech/medaka>). Manual indel correction was then performed as described previously for the coding regions of the nucleoprotein and glycoprotein genes (Gigante et al, 2020). WGS was performed on cDNA generated from total RNA using Maxima H-minus double-stranded cDNA synthesis kit (Thermo Fisher, Waltham, MA, USA) after DNase digestion using ezDNase (Thermo Fisher, Waltham, MA, USA) following manufacturer's protocols. cDNA was sequenced on a NovaSeq 6000 using the Illumina DNA prep kit following the manufacturer's recommendations using half reagent volumes (Illumina, San Diego, CA, USA).

At the Wadsworth lab, WGS was performed as described previously with minor modifications (Brunt et al, 2020). Sample RNA eluates were evaluated for quality control by rtRT-PCR, then quantified by Nanodrop spectrophotometry (Thermo Fisher, Waltham, MA, USA) and Agilent 2100 Bioanalyzer (Agilent Technologies, Santa Clara, CA, USA). Total RNA was enriched using Poly(A) mRNA magnetic isolation module and NEBNext Ultra II Directional RNA Prep Kit for Illumina (New England Biolabs, Ipswich, MA, USA). Adapters were ligated with NEBNext Multiplex Oligos for Illumina, and libraries were quantified using the NEBNext Library Quant kit for Illumina (New England Biolabs, Ipswich, MA, USA). Samples were pooled and run on the Illumina NextSeq 500/550 using a Mid Output kit v2.5 (Illumina, San Diego, CA, USA).

Lyssavirus rabies quantification

We used a modified version of the pan-lyssavirus rtRT-PCR assay (Supplementary Figure S1.; Wadhwa et al, 2017) and compared relative viral loads based on cycle threshold values (C_t). The reactions were run on a BioRad CFX96 real-time PCR System using the AgPath-ID One-Step rtRT-PCR kit (Thermo Fisher, Waltham, MA, USA). Each reaction contained 5 µL of template RNA (diluted 1:10 in nuclease-free water), 3.5 µL of nuclease-free water, 12.5 µL 2× RT-PCR Buffer, 1 µL 25X RT-PCR Enzyme Mix, 0.5 µL each of 20 µM

IPC β-actin forward and reverse primers and 20 µM LN34 forward and reverse primers, and 0.5 µL of 10 µM β-actin (HEX) and modified LN34 (FAM) probe. The thermocycling parameters were as follows: 30 min at 50°C, 10 min at 95°C, and 45 cycles of 1 s at 95°C, and 20 s at 56°C. Each sample was run in triplicate, and each PCR plate included a nontemplate negative control and RNA from a street RV (USDA Center for Veterinary Biologics, #92-5A) as a positive control. The rtRT-PCR results were evaluated using the BioRad CFX Maestro software package.

Phylogenetic and statistical analyses

The RV glycoprotein gene, protein, or genome sequences were aligned using MAFFT v.7.450 using the FFT-NS-I x1000 algorithm (Katoh et al, 2002; Katoh and Standley, 2013). Substitution models were determined based on LnL score from a model test performed in Mega7. Maximum clade credibility trees were estimated using BEAST v1.8.3 under GTR+G + I substitution model with two codon partitions (1 + 2 and 3), using an uncorrelated log normal relaxed clock and Bayesian skyline prior for the RV glycoprotein and WGS data. Additional clock and tree priors were tested. Tip dates were specified in years with a precision of 0.5 for the RV sequences analyzed (Supplementary Table S1).

An RV glycoprotein gene alignment containing representatives from major bat variants found in Arizona (Supplementary Table S2) was analyzed for evidence of selection in the Ef-W1 variant using branch-site models in the CODEML package in PAML 4.5 (Yang, 2007). Model A (includes codons under positive selection in the Ef-W1 variant, specified by NSSites = 2, model = 2, fixomega = 0) was compared to Model A1 (no positive selection allowed, specified by NSSites = 2, model = 2, fixomega = 1) by log likelihood test. Analyses were performed with a user tree generated using BEAST v1.8.3 under HKY + G + I substitution model, a strict clock and constant coalescent prior, CodonFreq = 2, and all ambiguous sites were removed. Sites where dN/dS > 1 were identified based on Bayes Empirical Bayes analysis using Pr(ω > 1) > 0.95 as a cutoff (Yang et al,

TABLE 1. RABID BATS AND MESOCARNIVORES FROM PUBLIC HEALTH AND ENHANCED RABIES SURVEILLANCE DURING 2021–2023 FROM NORTHERN ARIZONA, USA. THE RV VARIANT TYPING INFORMATION IS DESCRIBED WHERE AVAILABLE, OR CLARIFIED WHEN SAMPLES WERE NOT TYPED (NT)

Common name	Scientific name	Number rabid	RV variant	Year
Ringtail	<i>Bassariscus astutus</i>	1	Brazilian free-tailed bat	2021
Hooded skunk	<i>Mephitis macroura</i>	1	South-Central skunk	2021
Striped skunk	<i>Mephitis mephitis</i>	16	Ef-W1	2021
Striped skunk	<i>M. mephitis</i>	4	Ef-W1	2022
Striped skunk	<i>M. mephitis</i>	2	Ef-W1	2023
Gray fox	<i>Urocyon cinereoargenteus</i>	1	Ef-W1	2021
Pallid bat	<i>Antrozous pallidus</i>	1	nt	2023
Big brown bat	<i>Eptesicus fuscus</i>	2	Ef-W1	2021
Big brown bat	<i>E. fuscus</i>	1	Ef-W1	2022
Big brown bat	<i>E. fuscus</i>	4	Ef-W1 ^a	2023
Hoary bat	<i>Lasiurus cinereus</i>	1	Hoary bat	2023
Southwestern myotis	<i>Myotis auriculus</i>	1	Novel bat variant ^b	2023
Southwestern myotis	<i>M. auriculus</i>	1	Silver-haired bat	2023
Long-legged Myotis	<i>Myotis volans</i>	1	Ef-W1	2022

^aTwo cases confirmed with Ef-W1 RV variant and two cases were not typed.

^bNovel bat RV variant as described in literature by Condori et al. (2022).

Ef-W1, *Eptesicus fuscus*; RV, *Lyssavirus rabies*.

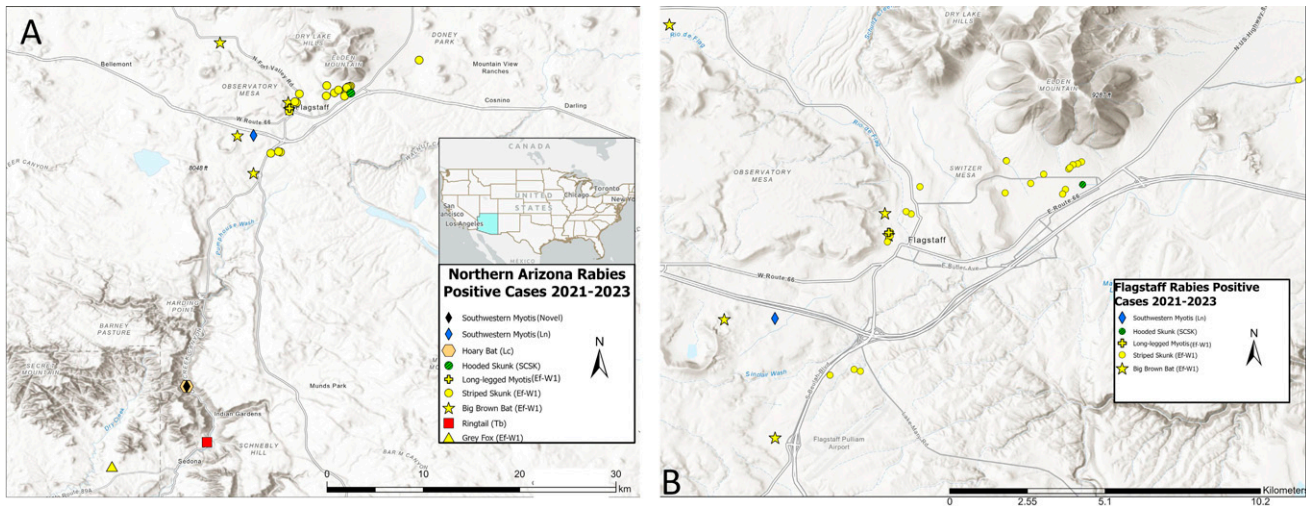


FIG. 1. Locations, host species, and RV variant typing among rabid animal cases in northern Arizona during 2021–2023 (A) and the subset reported from Flagstaff (B). Multiple bat RV variants were detected in mesocarnivores, including 22 cases of big brown bat (*E. fuscus*, Ef-W1) variant in striped skunks (*Mephitis mephitis*) and one case in a gray fox (*Urocyon cinereoargenteus*), compared to a single case each of the South-Central Skunk variant in a hooded skunk (*Mephitis macroura*) and a Brazilian free-tailed bat (*Tadarida brasiliensis*) variant in a ringtail (*Bassariscus astutus*). Multiple bat RV variants were described among rabid bats in northern Arizona during 2021–2023, including but not limited to Ef-W1 RV. Ef-W1, *Eptesicus fuscus*; RV, *Lyssavirus rabies*.

2005). Branches tested as the foreground lineage are depicted in Supplementary Figure S2.

Differences in rtRT-PCR detection of the two RV variants were evaluated for brain and salivary gland samples. The C_t values from both sample types were normalized using the $2^{-(\Delta\Delta C_t)}$ approach (Livak and Schmittgen, 2001; Supplementary Figure S3.). We log transformed $2^{-(\Delta\Delta C_t)}$ data to conform to a normal distribution based on the Shapiro–Wilk test (brain: $W = 0.98, p = 0.41$; salivary gland: $W = 0.93, p = 0.16$), and we tested for differences of transformed C_t value means between RV variants using

Welch’s unequal variances *t*-test in R v4.1.3, evaluated with $\alpha = 0.05$.

Results

A total of 22 cases of Ef-W1 RV variant was detected from striped skunks in northern Arizona during 2021–2023, in addition to one case in a gray fox during 2021 (Table 1, Fig. 1). Cases of Ef-W1 RV were detected from big brown bats in northern Arizona each year during 2021–2023, and one

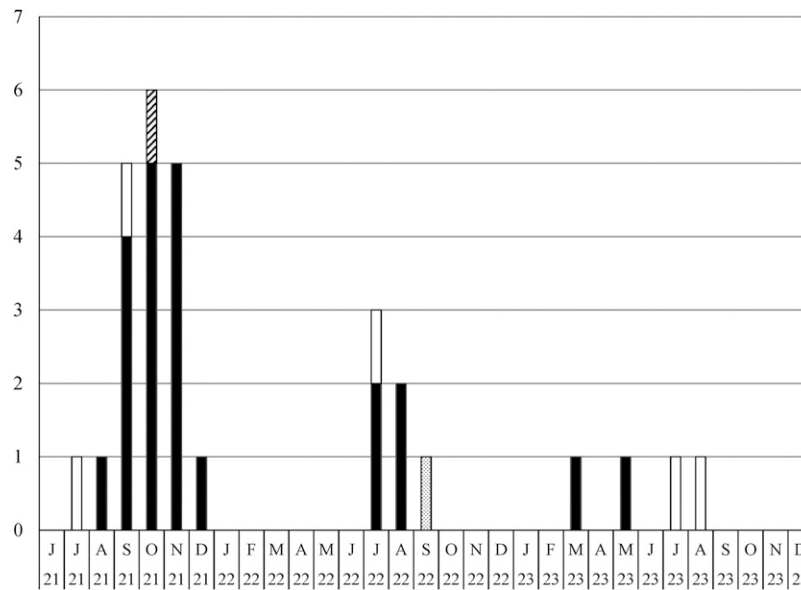


FIG. 2. The prevalence of big brown bat (Ef-W1) *Lyssavirus rabies* variant in northern Arizona during 2021–2023, based on public health and enhanced rabies surveillance. Cases were detected from big brown bats (white bars), a long-legged Myotis bat (*Myotis volans*; dotted hatch bar), striped skunks (*Mephitis mephitis*, black bars), and a gray fox (*Urocyon cinereoargenteus*, diagonal hatch bar). Ef-W1, *Eptesicus fuscus*.

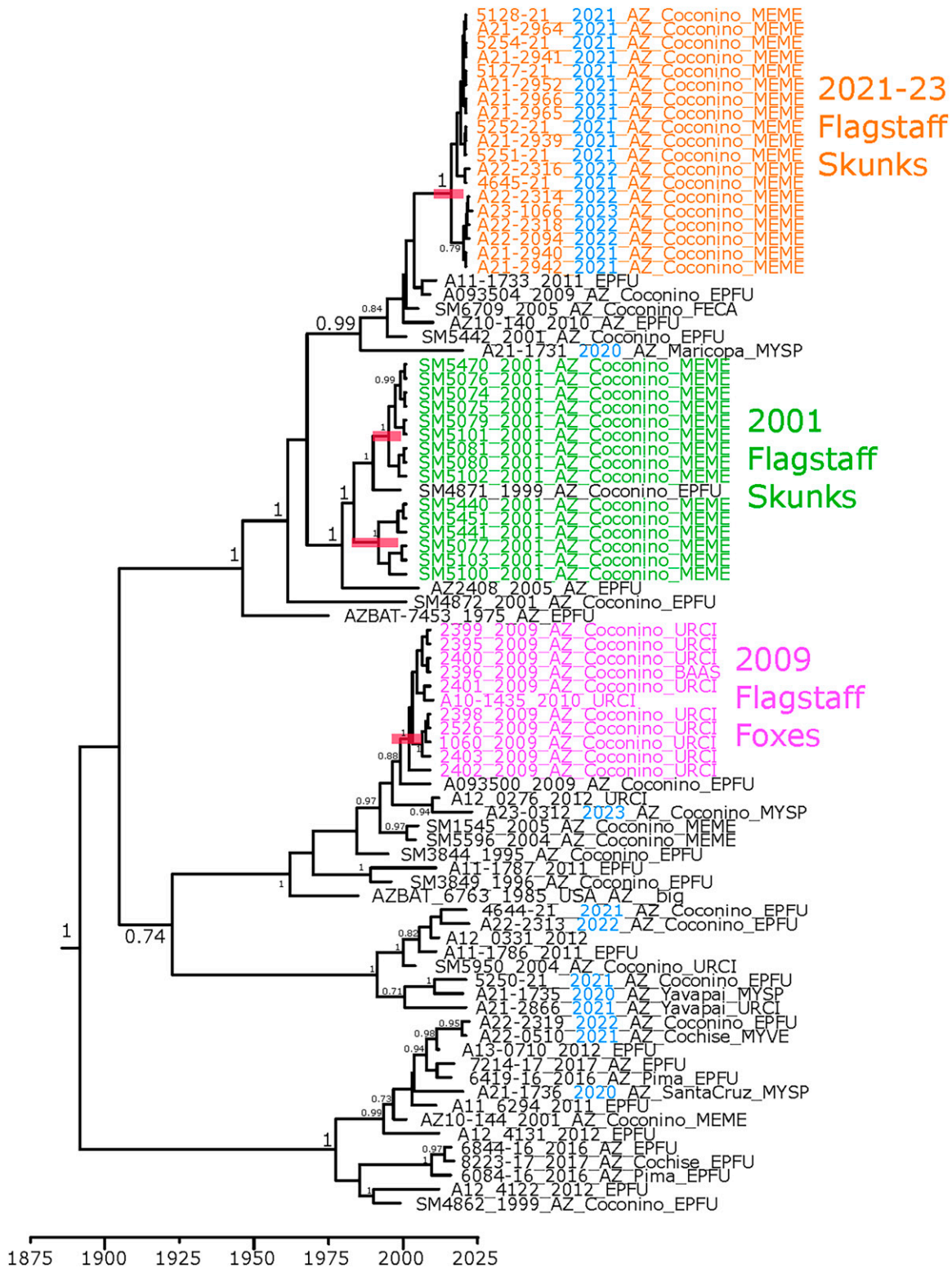


FIG. 3. Phylogenetic analysis of Ef-W1 RV sequences from Arizona, USA. Phylogenetic tree estimated from alignment of RV glycoprotein gene sequences. Posterior support values >0.7 are displayed on the nodes. Scale is in years. Blue coloring indicates sample collected since 2020. Host shift clades are highlighted by colored sample names. Sample names follow the format ISOLATE_YEAR_STATE_COUNTY_HOST, and the RV variant JQ685942 (EF-W2) was used as an outgroup to root the tree. Ef-W1, *Eptesicus fuscus*; EPFU, *Eptesicus fuscus*; FECA, *Felis catus*; MEME, *Mephitis mephitis*; MYSP, *Myotis* species; MYVE, *Myotis velifer*; RV, *Lyssavirus rabies*; URCI, *Urocyon cinereoargenteus*.

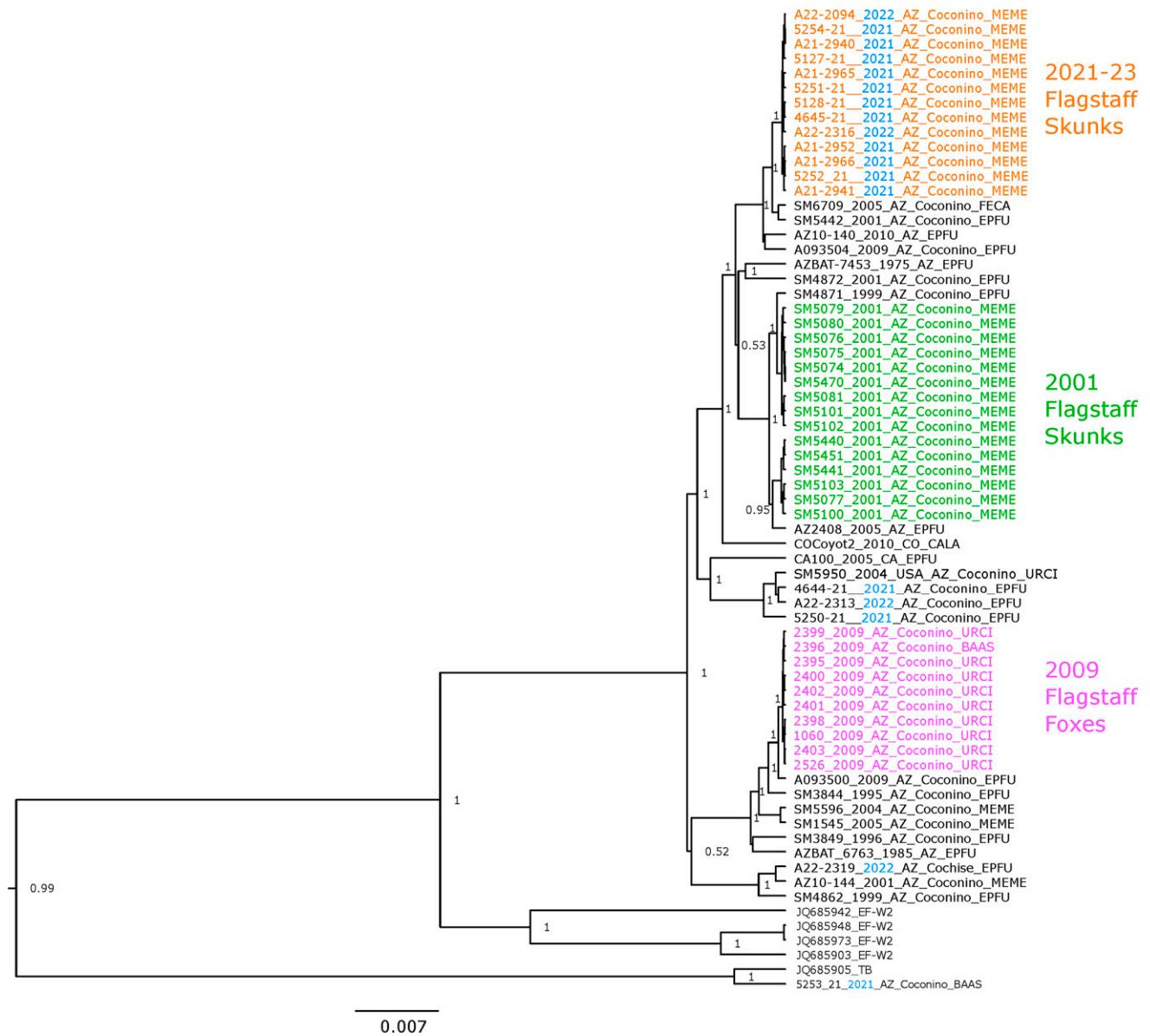


FIG. 4. Phylogenetic analysis of RV WGS of Ef-W1 variant from Arizona and other states, USA. Posterior support values >0.7 are displayed on the nodes. Scale is in years. The tree was rooted using South-Central skunk RV variant. Host shift clades are highlighted by colored sample names. Sample names follow the format ISOLATE_YEAR_STATE_COUNTY_HOST. BAAS, *Bassariscus astutus*; CALA, *Canis latrans*; Ef-W1, *Eptesicus fuscus*; EPFU, *Eptesicus fuscus*; FECA, *Felis catus*; MEME, *Mephitis mephitis*; MYSP, *Myotis* species; MYVE, *Myotis velifer*; RV, *Lyssavirus rabies*; URCI, *Urocyon cinereoargenteus*; WGS, whole genome sequences.

spillover infection was reported in a long-legged *Myotis* (*Myotis volans*) during 2022 (Table 1, Figs. 1 and 2). A single rabid ringtail (*Bassariscus astutus*) detected during October 2021 was infected with a Brazilian free-tailed bat (*Tadarida brasiliensis*) RV variant and one hooded skunk (*Mephitis macroura*) reported during September 2021 was infected with a South-Central skunk (SCSK) RV variant (Table 1, Fig. 1). Several other positive bats were detected in northern Arizona during 2023, infected with multiple bat RV variants (Table 1), including a novel bat RV described from New Mexico (Condori et al, 2022).

The index case of Ef-W1 RV in striped skunks was detected in August 2021, while the greatest monthly incidence of Ef-W1 RV cases was documented in northern Arizona during

September–November 2021 (Fig. 2). The majority of animals tested and rabid animals reported in northern Arizona during 2021–2023 were from USDA APHIS Wildlife Services ERS (Supplementary Table S3).

Phylogenetic reconstruction of relationships from Ef-W1 RV glycoprotein and WGS, including the prior outbreaks during 2001–2009, supported the independent emergence of the 2021–2023 outbreak (Figs. 3 and 4). The Ef-W1 sequences from skunks during 2021–2023 formed a monophyletic cluster that did not contain any of the Ef-W1 RV sequences isolated from bats during 2020–2023 (Figs. 3 and 4). The 2021–2023 outbreak of Ef-W1 in skunks was most closely related to sequences isolated from big brown bats in Arizona during 2001, 2010, and 2011 and an RV sequence from a cat (*Felis*

TABLE 2. AGE OF MRCA AND MUTATION RATE ESTIMATES FROM BEAST ANALYSIS OF LYSSAVIRUS RABIES WHOLE GENOME SEQUENCES SHOWN IN FIGURE 4. SEVERAL PARAMETERS WERE TESTED TO DETERMINE IF MUTATION RATE OR ESTIMATED DIVERGENCE TIME ESTIMATES WERE INFLUENCED BY PARAMETERS CHOSEN. MEAN AND 95% HPD (IN BRACKETS) ARE SHOWN. ESTIMATES PRODUCED FROM A SEPARATE ALIGNMENT OF 86 GLYCOPROTEIN GENES ARE ALSO SHOWN

Region	Whole genome		Whole genome		Whole genome		Glycoprotein gene	
	Strict	Constant coalescent	Uncorrelated log normal	Exponential	Uncorrelated log normal	Bayesian skyline	Uncorrelated log normal	Bayesian skyline
Substitution model	GTR+G+I		GTR+G+I		GTR+G+I		GTR+G+I	
Clock	5.7 × 10 ⁻⁵ [3.85E-5, 7.50E-5]	7.1 × 10 ⁻⁵ [4.3E-5, 10.0E-5]	7.4 × 10 ⁻⁵ [4.76E-5, 1.02E-4]	7.4 × 10 ⁻⁵ [4.76E-5, 1.02E-4]	6.5 × 10 ⁻⁵ [4.3E-5, 8.8E-5]	6.5 × 10 ⁻⁵ [4.3E-5, 8.8E-5]	8.7 × 10 ⁻⁵ [5.5E-5, 12.0E-5]	8.7 × 10 ⁻⁵ [5.5E-5, 12.0E-5]
Tree prior	1928 [1901, 1951]	1938 [1913, 1961]	1942 [1919, 1960]	1942 [1919, 1960]	1930 [1903, 1956]	1930 [1903, 1956]	1982 [1938, 1997]	1982 [1938, 1997]
Rate	1955 [1991, 1998]	1995 [1991, 1998]	1995 [1992, 1998]	1995 [1992, 1998]	1995 [1992, 1998]	1995 [1992, 1998]	1995 [1990, 1999]	1995 [1990, 1999]
ageMRCA (2001 skunks)	1994 [1989, 1997]	1994 [1989, 1998]	1995 [1990, 1999]	1995 [1990, 1999]	1995 [1990, 1998]	1995 [1990, 1998]	1991 [1983, 1998]	1991 [1983, 1998]
ageMRCA (2001a skunks)	2003 [2000, 2006]	2003 [2001, 2007]	2004 [2001, 2007]	2004 [2001, 2007]	2005 [2003, 2007]	2005 [2003, 2007]	2002 [1990, 2006]	2002 [1990, 2006]
ageMRCA (2001b skunks)	2015 [2011, 2018]	2015 [2012, 2019]	2016 [2012, 2019]	2016 [2012, 2019]	2016 [2012, 2019]	2016 [2012, 2019]	2016 [2010, 2020]	2016 [2010, 2020]
ageMRCA (2009 foxes)								
ageMRCA (2021 skunks)								

HPD, highest posterior density; MRCA, most recent common ancestor.

catus) in Coconino County in 2005. The 2021–2023 Ef-W1 RV sequences from skunks shared a common ancestor with sequences from two Ef-W1 RV host shifts into skunks in 2001. However, 2001 and 2021–2023 skunk sequences form monophyletic clades in all phylogenies, separated by RV sequences collected from bats and other animals (Figs. 3 and 4). The 2009 Ef-W1 RV outbreak in gray foxes was more distantly related to both the 2001 and 2021–2023 outbreak clades.

Timing estimates for the most recent common ancestor (MRCA) of the 2021–2023 cases were 2015 or 2016, based on WGS and glycoprotein phylogenetic trees (Fig. 3, Table 2). The 95% highest posterior density (HPD) region for the MRCA based on the WGS included estimates as early as 2011 and as recent as 2019, suggesting the introduction of Ef-W1 into skunks likely occurred several years prior to detection in 2021. The MRCA of two sister clades of Ef-W1 documented from the 2001 outbreak in skunks from Flagstaff was estimated to be circulating prior to 1960, with MRCA of each sister clade estimated around 1995 (Table 2), in agreement with previous analyses that the two 2001 sister clades represented independent introductions (Kuzmin et al, 2012). The MRCA for the 2009 outbreak of Ef-W1 in gray foxes was estimated to occur during the early 2000s. In all four host shift events, MRCA estimations preceded detection in the new host by at least 2–3 years (Table 2). The MRCA time estimates reported provide further evidence of independent evolution of the prior and current Ef-W1 RV outbreaks in mesocarnivores from northern Arizona.

We examined glycoprotein sequences to investigate whether there was evidence of adaptation in the Ef-W1 RV variant, both within the four host shift clusters, and more broadly, across sequences. All glycoprotein sequences from the 2021 skunk Ef-W1 cases were identical (0 amino acid differences, 0–2 nucleotide differences) (Fig. 5), as observed within the 2009 fox, 2001a skunk, and 2001b skunk outbreak clades (Fig. 5). Within the Ef-W1 RV, two unique amino acid changes were observed in the 2021 clade of skunks (M462I and S496P), in comparison to the 2001–2009 outbreaks, yet these mutations were also observed among sequences from 2001, 2009, and 2010 big brown bats and a 2005 cat from Coconino County (Fig. 5). No unique amino acid changes were shared across all three spillover clusters relative to other Ef-W1 RV sequences, and no unique sites were under positive selection within the four host shift clusters, within the lineage containing all host shift clusters, or across all Ef-W1. Amino acids 272S, 403V, and 503S exhibited evidence of positive selection in both Ef-W1 and Ef-W2 compared with other bat RV variant lineages [$P(\omega > 1) = 0.702, 0.679, \text{ and } 0.704$, respectively]. Whether these amino acid changes preadapt the virus for a host shift is not clear, as no host shifts have been reported for variant Ef-W2.

We detected RV by rtRT-PCR in all brain samples from rabid animals, whereas no RV was detected in brain samples from skunks with a negative rabies diagnosis (Table 3, Supplementary Table S4; skunks with negative RV diagnosis not shown). The mean RV C_t was 17.8 (range: 16.4–21.7) for the brains of 15 Ef-W1-positive skunks (Table 3) and 17.1 (range: 14.4–21.5) for the brains of 32 SCSK-positive skunks (Supplementary Table S4). A two-sided *t*-test for differences in mean 2^{-(ΔΔC_t)} brain C_t values between rabid striped skunks infected with Ef-W1 or SCSK RV variant(s)

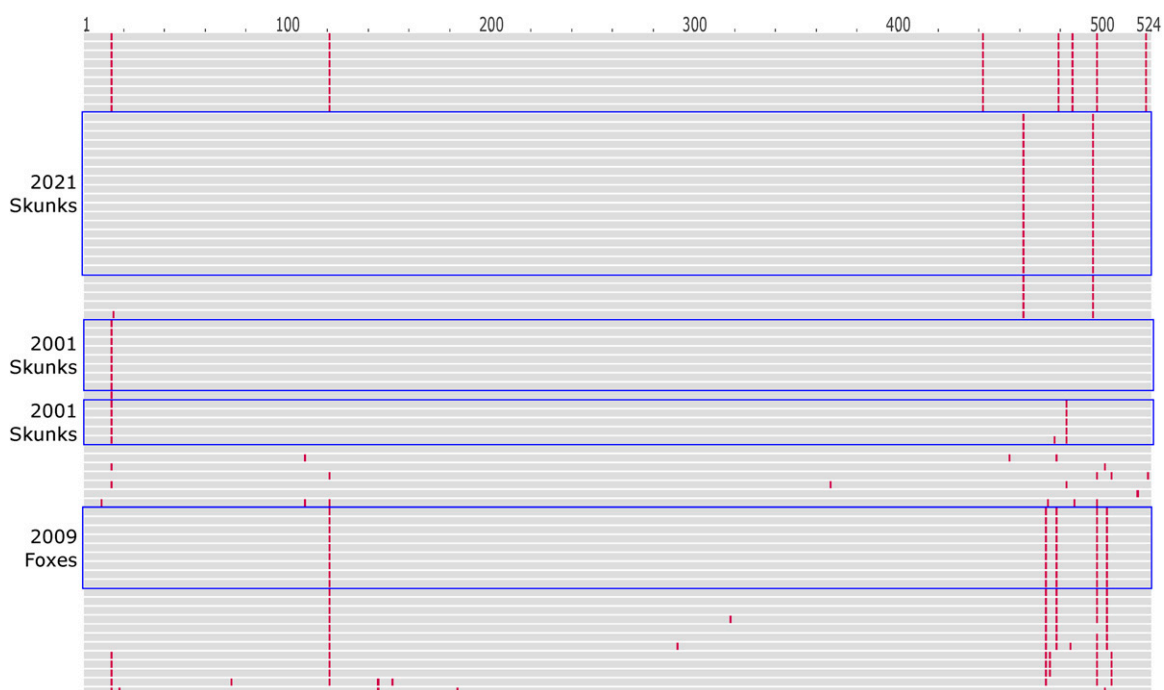


FIG. 5. Amino acid changes in the glycoprotein among Ef-W1 RV variant sequences shown in Figure 3. Each horizontal line represents one protein sequence. Amino acids identical to the RV glycoprotein sequence from GenBank accession JQ685956.1 (Arizona bat 1975) are shown in gray. Amino acid changes relative to JQ685956.1 are shown in red. Sequences from 2021, 2009, and 2001 Ef-W1 RV mesocarnivore host shift clusters are identified with blue boxes. Ef-W1, *Eptesicus fuscus*; RV, *Lyssavirus rabies*.

suggests a marginal difference ($t = 1.94$, $df = 19.2$, $p = 0.07$; Supplementary Figure S4).

We encountered rRT-PCR RV detection curves with atypical morphology from some salivary gland samples. Samples with atypical RV detection curves were retested with additional RNA (from 5 μ L to 8.5 μ L), yet the detection

curve morphology remained atypical. The salivary gland samples with atypical RV detection curves were scored as indeterminate for quantification, comprising two (13% of 15) Ef-W1 RV samples and six (19% of 32) SCSK RV samples. We detected RV in 9 of 12 (75%) mandibular salivary glands from rabid skunks infected with Ef-W1, with a mean C_t of 23.7

TABLE 3. THE MEAN CYCLE THRESHOLD VALUES (C_t) ACROSS REAL-TIME REVERSE TRANSCRIPTASE PCR TRIPPLICATE RUNS FOR THE DETECTION OF A BETA-ACTIN IPC AND *LYSSAVIRUS RABIES* RNA (mLN34) IN BRAIN AND MANDIBULAR SG TISSUES OF SKUNKS NATURALLY INFECTED WITH BIG BROWN BAT (*EPTESICUS FUSCUS*) *LYSSAVIRUS RABIES* VARIANT (EF-W1) IN COCONINO COUNTY DURING 2021–2023

Laboratory ID	Brain		Mandibular SG	
	Beta-actin mean (IPC)	mLN34 result	Beta-actin mean (IPC)	mLN34 result
AZ002	18.7	17.6	20.2	20.0
AZ004	17.4	16.5	19.1	20.7
AZ006	20.2	17.7	21.1	23.9
AZ007	20.7	17.2	27.0	Indeterminate
AZ008	21.4	17.3	22.5	17.0
AZ011	20.4	17.3	36.5 ^a	Indeterminate
AZ012	20.7	16.4	23.8	Not detected
AZ013	21.6	18.5	28.6	Not detected
AZ014	20.5	21.7	25.5	Not detected
AZ015	20.6	16.5	25.3	23.1
AZ017	23.8	19.5	30.9	26.3
AZ018	24.1	16.6	31.1	32.1
AZ019	23.7	18.0	32.6	Indeterminate
AZ022	20.2	19.3	27.9	28.7
AZ023	21.3	16.8	26.8	21.3

^aIPC value considered invalid test for RV detection, scored as indeterminate. Ef-W1, *Eptesicus fuscus*; IPC, internal positive control; RV, *Lyssavirus rabies*; SG, salivary gland.

(range: 17.0–32.1; Table 3), and from 9 of 26 (34%) mandibular salivary glands from rabid skunks infected with SCSK variant, with a mean C_t of 26.4 (range: 18.4–35.0; Supplementary Table S4). The IPC failed for one rabid skunk mandibular salivary gland sample infected with Ef-W1 RV variant, with RV detection scored as indeterminate (Table 3). A two-sided *t*-test for differences in mean $2^{-(\Delta\Delta C_t)}$ mandibular salivary gland C_t values between rabid striped skunks infected with Ef-W1 or SCSK RV variant(s) was not significant ($t = 1.56$, $df = 13.7$, $p = 0.14$; Supplementary Figure S5).

From nine skunks where Ef-W1 RV was detected in mandibular salivary glands, eight had sublingual gland tissue available for rRT-PCR testing and seven of the eight skunks also had RV detected in sublingual salivary glands (Supplementary Table S5). In contrast, the rRT-PCR test of mandibular salivary glands for one skunk (Ef-W1, AZ011; Table 3) failed on the beta-actin IPC, yet RV was detected from sublingual salivary glands (Supplementary Table S5). Parotid salivary gland tissues from 15 skunks infected with Ef-W1 were tested by rRT-PCR, but samples from three skunks were excluded due to atypical RV detection curves and indeterminate results, leaving five of 12 (42%) skunks with RV detected from the parotid salivary glands (i.e., four skunks with RV positive and one skunk with indeterminate mandibular gland results; Supplementary Table S5). Sublingual and parotid gland tissues from rabid skunks of northern Colorado, infected with SCSK RV, were not available for comparison.

Discussion

The reemergence of the Ef-W1 big brown bat RV in mesocarnivores from northern Arizona, USA, during 2021–2023 strengthens the evidence suggesting that this RV variant may be preadapted for spillover infections and host shifts (Kuzmin et al, 2012). The 2021–2023 outbreak in skunks shared a MRCA with singular detections of Ef-W1 spillover in a cat from 2005 and circulation of RV in big brown bats during 2009–2011, but the 2021–2023 outbreak was distinct from the clade(s) of Ef-W1 viruses that emerged in mesocarnivores in northern Arizona during 2001–2009. Results of this study suggest a high potential for onward transmission within striped skunk populations in this region. Salivary shedding of RV is a prerequisite for transmission by bite, yet RV excretion in the salivary glands of rabid skunks may be a transient phenomenon, depending on variation in RV dissemination from the central nervous system to and replication in peripheral tissues (Charlton et al, 1983; Charlton et al, 1987).

Regional studies of skunk RV variant epizootiology report an overwhelming majority of cases occurring in striped skunks (Dragoo et al, 2004; Oertli et al, 2009; Pepin et al, 2017). Given the context of the prior emergence of Ef-W1 RV in striped skunks and gray foxes in northern Arizona during 2001–2009 and nearly exclusive reporting of 2021–2023 cases in striped skunks, there is a valid reason for ERS targeting mesocarnivores in the region, although onward transmission may be more likely in striped skunks. An emerging RV variant in mesocarnivores is concerning to managers due to the known challenges of targeting skunks with cost-efficient control strategies, as reviewed elsewhere (Slate et al, 2009; Wohlers et al, 2018).

The close phylogenetic relationship of the cases during 2021–2023 suggests evidence of onward transmission within

skunks. The level of RV RNA copies in the brains of naturally infected skunks trended toward higher viral RNA loads for the emerging Ef-W1 RV compared to a skunk-adapted SCSK RV, yet there was also greater variability due to a smaller number of Ef-W1 RV infected skunks sampled. While the RV RNA copy levels from naturally infected skunk mandibular SGs were indistinguishable between the two RV variants, not all glands could be evaluated quantitatively in the comparison due to the presence of indeterminate results. Marston et al (2017) suggested that increased RV population genomic diversity within spillover hosts could result in a longer incubation time allowing viral loads and diversity to accumulate, increasing the chances for highly adapted genotypes to be transmitted to conspecifics. The trend toward greater Ef-W1 RV RNA in skunk brains, also supported by equivalent amounts of RV RNA in the salivary glands, may indicate either a high replication efficiency or a longer incubation period in the spillover host, despite our lack of evidence for positive selection on the reemerging Ef-W1 variant. One limitation with the salivary gland results may be individual variation among skunks in the disease progression at the time of submission for public health or ERS surveillance, and caution may also be warranted regarding the inference to RV shedding and transmission risk from salivary glands, given greater rates of RV isolation previously reported from the salivary glands of naturally infected skunks in northern Colorado (Jimenez et al, 2019). Future comparisons between rRT-PCR and RV isolation from salivary glands, for contextualizing RV shedding potential, are recommended, and deep sequencing of salivary glands may lend insight to the processes of RV evolution and novel host adaptation. Campaigns to enhance public awareness, education, outreach, and enhanced surveillance activities are warranted in the southwestern USA, for timely detection and response to emerging and reemerging bat RV variants in mesocarnivores, with impacts for human and animal health.

Acknowledgments

The authors thank T. Spraker and M. Selleck for assistance with the samples from northern Colorado. The authors also thank A. Barbee for technical assistance with the sample curation, processing, and data collection.

Authors' Contribution

All authors contributed substantively to the report, and all authors approve of the findings described therein.

Author Disclosure Statement

The authors have no conflicts of interest to declare with respect to the contents or findings reported. The findings and conclusions in this report are those of the authors and do not necessarily represent the views of the Centers for Disease Control and Prevention, the US Department of Agriculture, nor any partnering agencies.

Funding Information

This research was supported by the US Department of Agriculture, Wildlife Services, National Rabies Management Program.

Supplementary Material

Supplementary Data S1
 Supplementary Figure S1
 Supplementary Figure S2
 Supplementary Figure S3
 Supplementary Figure S4
 Supplementary Figure S5
 Supplementary Table S1
 Supplementary Table S2
 Supplementary Table S3
 Supplementary Table S4
 Supplementary Table S5

References

- Badrane H, Tordo N. Host switching in Lyssavirus history from the Chiroptera to the Carnivora orders. *J Virol* 2001;75(17): 8096–8104; doi: 10.1128/jvi.75.17.8096-8104.2001
- Blanton JD, Palmer D, Rupprecht CE. Rabies surveillance in the United States during 2009. *J Am Vet Med Assoc* 2010; 237(6):646–657; doi: 10.2460/javma.237.6.646
- Borucki MK, Chen-Harris H, Lao V, et al. Ultra-deep sequencing of intra-host rabies virus populations during cross-species transmission. *PLoS Negl Trop Dis* 2013;7(11):e2555; doi: 10.1371/journal.pntd.0002555
- Brunt S, Solomon H, Leavitt H, et al. Origin of 3 rabid terrestrial animals in raccoon rabies virus-free zone, Long Island, New York, USA, 2016–2017. *Emerg Infect Dis* 2020;26(6): 1315–1319; doi: 10.3201/eid2606.191700
- Carey AB, McLean RG. The ecology of rabies: Evidence of co-adaptation. *J Appl Ecol* 1983;20(3):777–800; doi: 10.2307/2403126
- Charlton KM, Casey GA, Campbell JB. Experimental rabies in skunks: Mechanisms of infection of the salivary glands. *Can J Comp Med* 1983;47(3):363–369.
- Charlton KM, Casey GA, Campbell JB. Experimental rabies in skunks: Immune response and salivary gland infection. *Comp Immunol Microbiol Infect Dis* 1987;10(3-4):227–235; doi: 10.1016/0147-9571(87)90033-6
- Childs JE, Richt JA, Mackenzie JS. Introduction: Conceptualizing and partitioning the emergence process of zoonotic viruses from wildlife to humans. In: *Wildlife and Emerging Zoonotic Diseases: The biology, circumstances, and consequences of cross-species transmission*, Vol. 315. (Childs JE, Mackenzie JS, Richt JA., eds.) *Curr Top Microbiol Immunol*; Springer; 2007, pp. 1–31; doi: 10.1007/978-3-540-70962-6_1
- Condori RE, Aragon A, Breckenridge M, et al. Divergent rabies virus variant of probable bat origin in 2 gray foxes, New Mexico, USA. *Emerg Infect Dis* 2022;28(6):1137–1145; doi: 10.3201/eid2806.211718
- Daoust PY, Wandeler AI, Casey GA. Cluster of rabies cases of probable bat origin among red foxes in Prince Edward Island, Canada. *J Wildl Dis* 1996;32(2):403–406; doi: 10.7589/0090-3558-32.2.403
- Dettinger L, Gigante CM, Sellard M, et al. Detection of apparent early rabies infection by LN34 pan-lyssavirus real-time RT-PCR assay in Pennsylvania. *Viruses* 2022;14(9):1845; doi: 10.3390/v14091845
- Dragoo JW, Matthes DK, Aragon A, et al. Identification of skunk species submitted for rabies testing in the desert southwest. *J Wildl Dis* 2004;40(2):371–376; doi: 10.7589/0090-3558-40.2.371
- Fisher CR, Streicker DG, Schnell MJ. The spread and evolution of rabies virus: Conquering new frontiers. *Nat Rev Microbiol* 2018;16(4):241–255; doi: 10.1038/nrmicro.2018.11
- Gigante CM, Yale G, Condori RE, et al. Portable rabies virus sequencing in canine rabies endemic countries using the Oxford Nanopore MinION. *Viruses* 2020;12(11):1255; doi: 10.3390/v12111255
- Gilbert A. Rabies virus vectors and reservoir species. *Rev Sci Tech* 2018;37(2):371–384; doi: 10.20506/rst.37.2.2808
- Jackson AC. Pathogenesis. In: *Rabies: Scientific Basis of the Disease and its Management*, 4th ed. (Fooks AR, Jackson AC. eds.) Academic Press. 2020; pp. 303–345; doi: 10.1016/B978-0-12-818705-0.00009-1
- Jacquot M, Wallace MA, Streicker DG, et al. Geographic range overlap rather than phylogenetic distance explains rabies virus transmission among closely related bat species. *Viruses* 2022;14(11):2399; doi: 10.3390/v14112399
- Jimenez I, Spraker T, Anderson J, et al. Isolation of rabies virus from the salivary glands of wild and domestic carnivores during a skunk rabies epizootic. *J Wildl Dis* 2019;55(2):473–476; doi: 10.7589/2018-05-127
- Katoh K, Standley DM. MAFFT multiple sequence alignment software version 7: Improvements in performance and usability. *Mol Biol Evol* 2013;30(4):772–780; doi: 10.1093/molbev/mst010
- Katoh K, Misawa K, Kuma KI, et al. MAFFT: A novel method for rapid multiple sequence alignment based on fast Fourier transform. *Nucleic Acids Res* 2002;30(14):3059–3066; doi: 10.1093/nar/gkf436
- Kuzmin I, Shi M, Orciari L, et al. Molecular inferences suggest multiple host shifts of rabies viruses from bats to mesocarnivores in Arizona during 2001–2009. *PLoS Pathog* 2012;8(6): e1002786; doi: 10.1371/journal.ppat.1002786
- Leslie MJ, Messenger S, Rohde RE, et al. Bat-associated rabies virus in skunks. *Emerg Infect Dis* 2006;12(8):1274–1277; doi: 10.3201/eid1208.051526
- Livak KJ, Schmittgen TD. Analysis of relative gene expression data using real-time quantitative PCR and the 2^{-ΔΔCt} method. *Methods* 2001;25(4):402–408; doi: 10.1006/meth.2001.1262
- Marston DA, Horton DL, Nunez J, et al. Genetic analysis of a rabies virus host shift event reveals within-host viral dynamics in a new host. *Virus Evol* 2017;3(2):vex038; doi: 10.1093/ve/vex038
- Mollentze N, Streicker DG. Viral zoonotic risk is homogenous among taxonomic orders of mammalian and avian reservoir hosts. *Proc Natl Acad Sci U S A* 2020;117(17):9423–9430; doi: 10.1073/pnas.1919176117
- Mollentze N, Streicker DG, Murcia PR, et al. Virulence mismatches in index hosts shape the outcomes of cross-species transmission. *Proc Natl Acad Sci U S A* 2020;117(46): 28859–28866; doi: 10.1073/pnas.2006778117
- Nadin-Davis SA, Sheen M, Wandeler AI. Development of real-time reverse transcriptase polymerase chain reaction methods for human rabies diagnosis. *J Med Virol* 2009;81(8): 1484–1497; doi: 10.1002/jmv.21547
- Oertli EH, Wilson PJ, Hunt PR, et al. Epidemiology of rabies in skunks in Texas. *J Am Vet Med Assoc* 2009;234(5):616–620; doi: 10.2460/javma.234.5.616
- Patrick E, Bjorklund B, Kirby JD, et al. Enhanced rabies surveillance using a direct rapid immunohistochemical test. *J Vis Exp* 2019;146(146):e59416; doi: 10.3791/59416
- Pepin KM, Davis AJ, Streicker DG, et al. Predicting spatial spread of rabies in skunk populations using surveillance data

- reported by the public. *PLoS Negl Trop Dis* 2017;11(7): e0005822; doi: 10.1371/journal.pntd.0005822
- Plowright RK, Parrish CR, McCallum H, et al. Pathways to zoonotic spillover. *Nat Rev Microbiol* 2017;15(8):502–510; doi: 10.1038/nrmicro.2017.45
- Ronald GP, Powell J, Raj P, et al. Centers for Disease Control and Prevention. Protocol for postmortem diagnosis of rabies in animals by direct fluorescent antibody testing: A minimum standard for rabies diagnosis in the United States. Atlanta, GA; 2003. Available from: <https://www.cdc.gov/rabies/pdf/rabiesdfaspv2.pdf> [Last accessed: April 29, 2024].
- Rupprecht CE, Turmelle AS, Kuzmin IV. A perspective on lyssavirus emergence and perpetuation. *Curr Opin Virol* 2011; 1(6):662–670; doi: 10.1016/j.coviro.2011.10.014
- Rupprecht CE, Van Pelt LI, Davis AD, et al. Use of a direct, rapid immunohistochemical test for diagnosis of rabies virus in bats. *Zoonotic Diseases* 2022;2(1):1–8; doi: 10.3390/zoonoticdis2010001
- Slate D, Algeo TP, Nelson KM, et al. Oral rabies vaccination in North America: Opportunities, complexities, and challenges. *PLoS Negl Trop Dis* 2009;3(12):e549; doi: 10.1371/journal.pntd.0000549
- Smith JS. Rabies virus epitopic variation: Use in ecologic studies. *Adv Virus Res* 1989;36:215–253; doi: 10.1016/S0065-3527(08)60586-2
- Streicker DG, Turmelle A, Vonhof M, et al. Host phylogeny constrains cross-species emergence and establishment of rabies virus in bats. *Science* 2010;329(5992):676–679; doi: 10.1126/science.1188836
- Streicker DG, Biek R. Evolution of rabies virus. In: *Rabies: Scientific Basis of the Disease and its Management*, 4th ed. (Fooks AR, Jackson AC, eds.) Academic Press. 2020; pp. 83–101; doi: 10.1016/B978-0-12-818705-0.00003-0
- Streicker DG, Altizer SM, Velasco-Villa A, et al. Variable evolutionary routes to host establishment across repeated rabies virus host shifts among bats. *Proc Natl Acad Sci U S A* 2012; 109(48):19715–19720; doi: 10.1073/pnas.1203456109
- Troupin C, Dacheux L, Tanguy M, et al. Large-scale phylogenomic analysis reveals the complex evolutionary history of rabies virus in multiple carnivore hosts. *PLoS Pathog* 2016; 12(12):e1006041; doi: 10.1371/journal.ppat.1006041
- Wadhwa A, Wilkins K, Gao J, et al. A pan-lyssavirus taqman real-time RT-PCR assay for the detection of highly variable rabies virus and other lyssaviruses. *PLoS Negl Trop Dis* 2017;11(1):e0005258; doi: 10.1371/journal.pntd.0005258
- Wohlers A, Lankau EW, Oertli EH, et al. Challenges to controlling rabies in skunk populations using oral rabies vaccination: A review. *Zoonoses Public Health* 2018;65(4):373–385; doi: 10.1111/zph.12471
- Yang Z. PAML 4: Phylogenetic analysis by maximum likelihood. *Mol Biol Evol* 2007;24(8):1586–1591; doi: 10.1093/molbev/msm088
- Yang Z, Wong WS, Nielsen R. Bayes empirical bayes inference of amino acid sites under positive selection. *Mol Biol Evol* 2005;22(4):1107–1118; doi: 10.1093/molbev/msi097

Address correspondence to:

Amy T. Gilbert
United States Department of Agriculture
Animal and Plant Health Inspection Service
Wildlife Services
National Wildlife Research Center
Fort Collins, CO
USA

E-mail: amy.t.gilbert@usda.gov

1 Supplemental Material

2 S1 Data

3 *Lyssavirus rabies RNA isolation*

4 At the Wadsworth laboratory, total RNA was extracted from approximately 3x3 mm
5 pieces of tissue suspended in 1 mL of minimum essential medium. Suspensions were briefly
6 vortexed, then a 200 µL subsample was lysed and extracted with QIAasympphony (Qiagen,
7 Hilden, Germany) using the DSP Virus/Pathogen kit following the manufacturer's instructions
8 (Dupuis et al, 2015). At the CDC laboratory, total RNA was extracted from brain samples using
9 Trizol reagent and Directzol kit (Zymo Research, Irvine, CA, USA), as described previously
10 (Gigante et al, 2018). At the USDA laboratory in Fort Collins, Colorado total RNA for rtRT-
11 PCR was extracted from brain and mandibular salivary gland samples using the Zymo Research
12 *Quick-DNA/RNA Miniprep Plus Kit* following the manufacturer's protocol (Zymo Research,
13 Irvine, CA, USA). Brain samples were homogenized at 4 m/s for 30 seconds using ZR
14 BashingBead Lysis Tubes (Zymo Research, Irvine, CA, USA) and incubated at room
15 temperature for 30 minutes prior to extraction. Salivary glands were homogenized at 4 m/s in 30
16 second increments for a total of 2 minutes using 2 mm ZR BashingBead Lysis Tubes and
17 incubated at room temperature for 30 minutes.

18

19 References

20 Dupuis M, Brunt S, Appler K, et al. Comparison of automated quantitative reverse transcription-
21 PCR and direct fluorescent-antibody detection for routine rabies diagnosis in the United
22 States. *J Clin Microbiol* 2015;53(9):2983-2989.

- 23 Gigante CM, Dettinger L, Powell JW, et al. Multi-site evaluation of the LN34 pan-lyssavirus
24 real-time RT-PCR assay for post-mortem rabies diagnostics. PloS One
25 2018;13(5):e0197074.

26 S1 Table List of *Lyssavirus rabies* sequences analyzed from bats and mesocarnivores in Arizona.

Isolate	Accession	Year	City	County	State	Collection date	Host species
1060	JQ685908	2009	Flagstaff	Coconino	AZ	NA	<i>Urocyon cinereoargenteus</i>
2395	JQ685972	2009	Flagstaff	Coconino	AZ	NA	<i>Urocyon cinereoargenteus</i>
2396	JQ685937	2009	Flagstaff	Coconino	AZ	NA	<i>Bassariscus astutus</i>
2398	JQ685892	2009	Flagstaff	Coconino	AZ	NA	<i>Urocyon cinereoargenteus</i>
2399	JQ685939	2009	Flagstaff	Coconino	AZ	NA	<i>Urocyon cinereoargenteus</i>
2400	JQ685912	2009	Flagstaff	Coconino	AZ	NA	<i>Urocyon cinereoargenteus</i>
2402	JQ685896	2009	Flagstaff	Coconino	AZ	NA	<i>Urocyon cinereoargenteus</i>
2403	JQ685928	2009	Flagstaff	Coconino	AZ	NA	<i>Urocyon cinereoargenteus</i>
2526	JQ685976	2009	Flagstaff	Coconino	AZ	NA	<i>Urocyon cinereoargenteus</i>
A093500	JQ685898	2009	Flagstaff	Coconino	AZ	NA	<i>Eptesicus fuscus</i>
A093504	JQ685950	2009	Flagstaff	Coconino	AZ	NA	<i>Eptesicus fuscus</i>
A21-1731	PP386045/ PP386032	2020	NA	Maricopa	AZ	6/5/2020	<i>Myotis</i>

A21-1735	PP386053/ PP386039	2020	NA	Yavapai	AZ	9/18/2020	Myotis
A21-1736	PP386055/ PP386037	2020	NA	Santa Cruz	AZ	10/1/2020	Myotis
A21-2866	PP386052/ PP386040	2021	Sedona	Yavapai	AZ	10/8/2021	Urocyon cinereoargenteus
A21-2939	PP386049/ PP386034	2021	Flagstaff	Coconino	AZ	10/18/2021	Mephitis mephitis
A21-2940	PP386025	2021	Flagstaff	Coconino	AZ	10/25/2021	Mephitis mephitis
A21-2941	PP386024	2021	Flagstaff	Coconino	AZ	10/26/2021	Mephitis mephitis
A21-2942	PP386048/ PP386036	2021	Flagstaff	Coconino	AZ	11/10/2021	Mephitis mephitis
A21-2952	PP386023	2021	Flagstaff	Coconino	AZ	11/22/2021	Mephitis mephitis
A21-2964	PP386047/ PP386033	2021	Flagstaff	Coconino	AZ	12/1/2021	Mephitis mephitis
A21-2965	PP386027	2021	Flagstaff	Coconino	AZ	11/19/2021	Mephitis mephitis

A21-2966	PP386026	2021	Flagstaff	Coconino	AZ	11/20/2021	Mephitis mephitis
A22-0510	PP386054/ PP386038	2021	NA	Cochise	AZ	8/30/2021	Myotis velifer
A22-2094	PP386029	2022	Flagstaff	Coconino	AZ	7/14/2022	Mephitis mephitis
A22-2313	PP386030	2022	Flagstaff	Coconino	AZ	7/20/2022	Eptesicus fuscus
A22-2314	PP386046/ PP386042	2022	Flagstaff	Coconino	AZ	7/26/2022	Mephitis mephitis
A22-2316	PP386028	2022	Flagstaff	Coconino	AZ	8/15/2022	Mephitis mephitis
A22-2318	PP386050/ PP386043	2022	Flagstaff	Coconino	AZ	8/22/2022	Mephitis mephitis
A22-2319	PP386031	2022	Sierra Vista	Cochise	AZ	7/6/2022	Eptesicus fuscus
A23-0312	PP386051/ PP386041	2023	Flagstaff	Coconino	AZ	9/20/2022	Myotis volans
AZ10-140	JQ685961	2010	Flagstaff	Coconino	AZ	NA	Eptesicus fuscus
AZ10-144	JQ685951	2001	Flagstaff	Coconino	AZ	NA	Mephitis mephitis
AZ2408	JQ685926	2005	Flagstaff	Coconino	AZ	NA	Eptesicus fuscus

AZBAT-6763	JQ685913	1985	NA	NA	AZ	NA	Eptesicus fuscus
AZBAT-7453	JQ685956	1975	NA	NA	AZ	NA	Eptesicus fuscus
4644-21	PP447337	2021	Flagstaff	Coconino	AZ	7/26/2021	Eptesicus fuscus
4645-21	PP447338	2021	Flagstaff	Coconino	AZ	8/5/2021	Mephitis mephitis
5127-21	PP447334	2021	Flagstaff	Coconino	AZ	9/18/2021	Mephitis mephitis
5128-21	PP447341	2021	Flagstaff	Coconino	AZ	9/19/2021	Mephitis mephitis
5250-21	PP447340	2021	Flagstaff	Coconino	AZ	9/9/2021	Eptesicus fuscus
5251-21	PP447333	2021	Flagstaff	Coconino	AZ	9/29/2021	Mephitis mephitis
5252-21	PP447335	2021	Flagstaff	Coconino	AZ	9/30/2021	Mephitis mephitis
5254-21	PP447336	2021	Flagstaff	Coconino	AZ	10/7/2021	Mephitis mephitis
2401	JQ685934	2009	Flagstaff	Coconino	AZ	NA	Urocyon cinereoargenteus
AZBAT-65094	JQ685942	1981	NA	NA	AZ	NA	Eptesicus fuscus
A11-1733	JX871862	2011	NA	NA	AZ	NA	Eptesicus fuscus
A11-1786	JX871875	2011	NA	NA	AZ	NA	Eptesicus fuscus
A11-1787	JX871876	2011	NA	NA	AZ	NA	Eptesicus fuscus
A10_1435	KC791849	2010	NA	NA	NA	1/1/2010	Urocyon cinereoargenteus

A11_6294	KC792036	2011	NA	NA	NA	1/1/2011	Unspecified bat
A12_0276	KC792049	2012	NA	NA	NA	1/1/2012	Urocyon cinereoargenteus
A12_0331	KC792052	2012	NA	NA	NA	1/1/2012	Unspecified bat
A12_4122	KC792129	2012	NA	NA	NA	1/1/2012	Eptesicus fuscus
A12_4128	KC792132	2012	NA	NA	NA	1/1/2012	Eptesicus fuscus
A12_4131	KC792133	2012	NA	NA	NA	1/1/2012	Eptesicus fuscus
A13-0710	KJ174675	2012	NA	NA	NA	NA	Eptesicus fuscus
6084-16	PP681423	2016	Tucson	Pima	AZ	7/29/2016	Eptesicus fuscus
6419-16	PP681420/ PP681422	2016	Tucson	Pima	AZ	9/3/2016	Eptesicus fuscus
6844-16	PP681417/ PP681425	2016	NA	Santa Cruz	AZ	9/30/2016	Eptesicus fuscus
7214-17	PP681419/ PP681421	2017	NA	Cochise	AZ	8/2/2017	Eptesicus fuscus
8223-17	PP681418/ PP681424	2017	Bisbee	Cochise	AZ	9/22/2017	Eptesicus fuscus

SM1545	JQ685941	2005	Flagstaff	Coconino	AZ	NA	Mephitis mephitis
SM3844	JQ685974	1995	Flagstaff	Coconino	AZ	NA	Eptesicus fuscus
SM3849	JQ685907	1996	Flagstaff	Coconino	AZ	NA	Eptesicus fuscus
SM4862	JQ685946	1999	Flagstaff	Coconino	AZ	NA	Eptesicus fuscus
SM4871	JQ685923	1999	Flagstaff	Coconino	AZ	NA	Eptesicus fuscus
SM4872	JQ685960	2001	Flagstaff	Coconino	AZ	NA	Eptesicus fuscus
SM5074	JQ685935	2001	Flagstaff	Coconino	AZ	NA	Mephitis mephitis
SM5075	JQ685949	2001	Flagstaff	Coconino	AZ	NA	Mephitis mephitis
SM5076	JQ685932	2001	Flagstaff	Coconino	AZ	NA	Mephitis mephitis
SM5077	JQ685911	2001	Flagstaff	Coconino	AZ	NA	Mephitis mephitis
SM5079	JQ685893	2001	Flagstaff	Coconino	AZ	NA	Mephitis mephitis
SM5080	JQ685927	2001	Flagstaff	Coconino	NA	NA	Mephitis mephitis
SM5081	JQ685904	2001	Flagstaff	Coconino	AZ	NA	Mephitis mephitis
SM5100	JQ685940	2001	Flagstaff	Coconino	AZ	NA	Mephitis mephitis
SM5101	JQ685958	2001	Flagstaff	Coconino	AZ	NA	Mephitis mephitis
SM5102	JQ685906	2001	Flagstaff	Coconino	AZ	NA	Mephitis mephitis

SM5103	JQ685930	2001	Flagstaff	Coconino	AZ	NA	Mephitis mephitis
SM5440	JQ685969	2001	Flagstaff	Coconino	AZ	NA	Mephitis mephitis
SM5441	JQ685962	2001	Flagstaff	Coconino	AZ	NA	Mephitis mephitis
SM5442	JQ685897	2001	Flagstaff	Coconino	AZ	NA	Eptesicus fuscus
SM5451	JQ685959	2001	Flagstaff	Coconino	AZ	NA	Mephitis mephitis
SM5470	JQ685966	2001	Flagstaff	Coconino	AZ	NA	Mephitis mephitis
SM5596	JQ685964	2004	Flagstaff	Coconino	AZ	NA	Mephitis mephitis
SM5950	JQ685933	2004	Flagstaff	Coconino	AZ	NA	Urocyon cinereoargenteus
SM6709	JQ685945	2005	Flagstaff	Coconino	AZ	NA	Felis catus
A23-1066	PP386044/ PP386035	2023	Flagstaff	Coconino	AZ	3/28/2023	Mephitis mephitis

S2 Table List of *Lyssavirus rabies* glycoprotein sequence alignment representatives from major bat RV variants found in Arizona.

ID	Year	City	County	State	Collection date	Host species	Accession
1060_2009_USA_AZ__gray	2009	Flagstaff	Coconino	AZ	NA	Urocyon cinereoargenteus	JQ685908
2395_2009_USA_AZ__gray	2009	Flagstaff	Coconino	AZ	NA	Urocyon cinereoargenteus	JQ685972
2396_2009_USA_AZ__ring-tailed	2009	Flagstaff	Coconino	AZ	NA	Bassariscus astutus	JQ685937
2398_2009_USA_AZ__gray	2009	Flagstaff	Coconino	AZ	NA	Urocyon cinereoargenteus	JQ685892
2399_2009_USA_AZ__gray	2009	Flagstaff	Coconino	AZ	NA	Urocyon cinereoargenteus	JQ685939
2400_2009_USA_AZ__gray	2009	Flagstaff	Coconino	AZ	NA	Urocyon cinereoargenteus	JQ685912
2401_2009_USA_AZ_Coconino_gray	2009	Flagstaff	Coconino	AZ	NA	Urocyon cinereoargenteus	JQ685934
2402_2009_USA_AZ__gray	2009	Flagstaff	Coconino	AZ	NA	Urocyon cinereoargenteus	JQ685896
2403_2009_USA_AZ__gray	2009	Flagstaff	Coconino	AZ	NA	Urocyon cinereoargenteus	JQ685928
2526_2009_USA_AZ__gray	2009	Flagstaff	Coconino	AZ	NA	Urocyon cinereoargenteus	JQ685976
A093500_2009_USA_AZ_Coconino_big	2009	Flagstaff	Coconino	AZ	NA	Eptesicus fuscus	JQ685898

A093504_2009_USA_AZ_Coconino_big	2009	Flagstaff	Coconino	AZ	NA	Eptesicus fuscus	JQ685950
A22-2313	2022	Flagstaff	Coconino	AZ	7/20/2022	Eptesicus fuscus	PP386030
A21-2940p	2021	Flagstaff	Coconino	AZ	10/25/2021	Mephitis mephitis	PP386025
A21-2941p	2021	Flagstaff	Coconino	AZ	10/26/2021	Mephitis mephitis	PP386024
A21-2965p	2021	Flagstaff	Coconino	AZ	11/19/2021	Mephitis mephitis	PP386027
AZ10_140_2010_USA_AZ__big	2010	Flagstaff	Coconino	AZ	NA	Eptesicus fuscus	JQ685961
AZ10-144_2001_USA_AZ_Coconino_striped	2001	Flagstaff	Coconino	AZ	NA	Mephitis mephitis	JQ685951
AZ2408_2005_USA_AZ__big	2005	Flagstaff	Coconino	AZ	NA	Eptesicus fuscus	JQ685926
AZBAT_6763_1985_USA_AZ__big	1985	NA	NA	AZ	NA	Eptesicus fuscus	JQ685913

AZBAT_7453_1975_USA_AZ__big	1975	NA	NA	AZ	NA	Eptesicus fuscus	JQ685956
CA100_2005_USA_CA__big	2005	NA	NA	CA	NA	Eptesicus fuscus	JQ685909
CO_Coyot_2_2010_USA_CO__coyote	2010	NA	NA	CO	NA	Canis latrans	JQ685917
Consensus_4644-21	2021	Flagstaff	Coconino	AZ	7/26/2021	Eptesicus fuscus	PP447337
Consensus_4645-21	2021	Flagstaff	Coconino	AZ	8/5/2021	Mephitis mephitis	PP447338
Consensus_5127-21	2021	Flagstaff	Coconino	AZ	9/18/2021	Mephitis mephitis	PP447334
Consensus_5128-21	2021	Flagstaff	Coconino	AZ	9/19/2021	Mephitis mephitis	PP447341
Consensus_5250-21	2021	Flagstaff	Coconino	AZ	9/9/2021	Eptesicus fuscus	PP447340
Consensus_5251-21	2021	Flagstaff	Coconino	AZ	9/29/2021	Mephitis mephitis	PP447333
Consensus_5252-21	2021	Flagstaff	Coconino	AZ	9/30/2021	Mephitis mephitis	PP447335
Consensus_5253-21	2021	Sedona	Coconino	AZ	10/7/2021	Bassaricus astutus	PP447339
Consensus_5254-21	2021	Flagstaff	Coconino	AZ	10/7/2021	Mephitis mephitis	PP447336
JQ685903_EF-W2	2004	NA	NA	CA	NA	Eptesicus fuscus	JQ685903
JQ685905_TB	2003	NA	NA	FL	NA	Tadarida brasiliensis	JQ685905

JQ685938_SCSK	2009	Flagstaff	Coconino	AZ	NA	<i>Mephitis mephitis</i>	JQ685938
JQ685942_EF-W2	1981	NA	NA	AZ	NA	<i>Eptesicus fuscus</i>	JQ685942
JQ685948_EF-W2	2010	NA	NA	OR	NA	<i>Urocyon cinereoargenteus</i>	JQ685948
JQ685973_EF-W2	2011	NA	NA	OR	NA	<i>Canis latrans</i>	JQ685973
SM1545_2005_USA_AZ_Coconino o_striped	2005	Flagstaff	Coconino	AZ	NA	<i>Mephitis mephitis</i>	JQ685941
SM3844_1995_USA_AZ_Coconino o_big	1995	Flagstaff	Coconino	AZ	NA	<i>Eptesicus fuscus</i>	JQ685974
SM3849_1996_USA_AZ_Coconino o_big	1996	Flagstaff	Coconino	AZ	NA	<i>Eptesicus fuscus</i>	JQ685907
SM4862_1999_USA_AZ_Coconino o_big	1999	Flagstaff	Coconino	AZ	NA	<i>Eptesicus fuscus</i>	JQ685946
SM4871_1999_USA_AZ_Coconino o_big	1999	Flagstaff	Coconino	AZ	NA	<i>Eptesicus fuscus</i>	JQ685923
SM4872_2001_USA_AZ_Coconino o_striped	2001	Flagstaff	Coconino	AZ	NA	<i>Eptesicus fuscus</i>	JQ685960

SM5074_2001_USA_AZ__striped	2001	Flagstaff	Coconino	AZ	NA	Mephitis mephitis	JQ685935
SM5075_2001_USA_AZ__striped	2001	Flagstaff	Coconino	AZ	NA	Mephitis mephitis	JQ685949
SM5076_2001_USA_AZ_Coconino_striped	2001	Flagstaff	Coconino	AZ	NA	Mephitis mephitis	JQ685932
SM5077_2001_USA_AZ_Coconino_striped	2001	Flagstaff	Coconino	AZ	NA	Mephitis mephitis	JQ685911
SM5079_2001_USA_AZ_Coconino_striped	2001	Flagstaff	Coconino	AZ	NA	Mephitis mephitis	JQ685893
SM5080_2001_USA_AZ__striped	2001	Flagstaff	Coconino	NA	NA	Mephitis mephitis	JQ685927
SM5081_2001_USA_AZ_Coconino_striped	2001	Flagstaff	Coconino	AZ	NA	Mephitis mephitis	JQ685904
SM5100_2001_USA_AZ_Coconino_striped	2001	Flagstaff	Coconino	AZ	NA	Mephitis mephitis	JQ685940
SM5101_2001_USA_AZ_Coconino_striped	2001	Flagstaff	Coconino	AZ	NA	Mephitis mephitis	JQ685958
SM5102_2001_USA_AZ__striped	2001	Flagstaff	Coconino	AZ	NA	Mephitis mephitis	JQ685906

SM5103_2001_USA_AZ__striped	2001	Flagstaff	Coconino	AZ	NA	Mephitis mephitis	JQ685930
SM5440_2001_USA_AZ_Coconino_striped	2001	Flagstaff	Coconino	AZ	NA	Mephitis mephitis	JQ685969
SM5441_2001_USA_AZ_Coconino_striped	2001	Flagstaff	Coconino	AZ	NA	Mephitis mephitis	JQ685962
SM5442_2001_USA_AZ_Coconino_big	2001	Flagstaff	Coconino	AZ	NA	Eptesicus fuscus	JQ685897
SM5451_2001_USA_AZ__striped	2001	Flagstaff	Coconino	AZ	NA	Mephitis mephitis	JQ685959
SM5470_2001_USA_AZ_Coconino_striped	2001	Flagstaff	Coconino	AZ	NA	Mephitis mephitis	JQ685966
SM5596_2004_USA_AZ_Coconino_striped	2004	Flagstaff	Coconino	AZ	NA	Mephitis mephitis	JQ685964
SM5950_2004_USA_AZ_Coconino_gray	2004	Flagstaff	Coconino	AZ	NA	Urocyon cinereoargenteus	JQ685933
SM6709_2005_USA_AZ_Coconino_cat	2005	Flagstaff	Coconino	AZ	NA	Felis catus	JQ685945

S3 Table. The number of samples tested and number diagnosed with *Lyssavirus rabies* (RV) from northern Arizona, USA, 2021-2023.

The number of RV positive animals is indicated by parentheses. Cases were reported as part of United States Department of Agriculture enhanced rabies surveillance (ERS) or state public health rabies surveillance.

Location	2021		2022		2023	
	Public health	ERS	Public health	ERS	Public health	ERS
Flagstaff, Coconino County	16 (3)	32 (17)	22 (1)	15 (5)	16 (2)	24 (5)
Sedona, Yavapai County	2 (0)	2 (1)	0 (0)	0 (0)	1 (1)	6 (2)
Totals	18 (3)	34 (18)	22 (1)	15 (5)	17 (3)	30 (7)

S4 Table The mean cycle threshold values (C_t) across real-time reverse transcriptase PCR triplicate runs for the detection of a beta-actin internal positive control (IPC) and *Lyssavirus rabies* RNA (mLN34) in brain and mandibular salivary gland (SG) tissues of skunks naturally infected with South-Central skunk variant in Northern Colorado during 2018-2019.

Laboratory ID	Brain		Mandibular SG	
	beta-actin mean (IPC)	mLN34 result	beta-actin mean (IPC)	mLN34 result
DX073	18.6	17.2	20.9	Not detected
DX074	18.5	15.9	22.3	Not detected
DX075	18.2	16.6	20.0	Indeterminate
DX076	19.0	16.8	18.3	18.4
DX078	25.4	21.5	33.2	34.3
DX079	19.6	17.7	31.8*	33.9*
DX081	20.4	18.4	19.1	Not detected
DX082	20.2	18.3	28.5	Not detected
DX083	20.3	17.2	29.7	Not detected
DX086	25.5	21.4	28.7	28.1

DX087	17.5	15.2	22.7	Not detected
DX088	23.2	17.3	30.7	35.0
DX089	18.7	17.8	22.8	Not detected
DX091	19.9	20.6	23.3	Not detected
DX092	19.4	18.4	23.1	Not detected
DX093	18.0	16.3	20.5	Indeterminate
DX094	30.4	18.6	26.2	Not detected
DX095	19.7	16.4	24.6	Indeterminate
DX096	17.3	15.0	22.4	23.8
DX097	18.1	16.1	22.5	25.4
DX099	18.0	15.5	26.0	Not detected
DX100	17.6	16.8	18.3	Not detected
DX101	17.7	16.0	18.6	Not detected
DX103	19.5	17.5	20.8	Not detected
DX104	17.3	17.1	18.8	19.7
DX105	17.4	15.4	22.3	Not detected

DX106	17.4	15.8	25.6	Indeterminate
DX107	18.1	17.3	22.1	Indeterminate
DX108	18.1	14.4	22.7	Indeterminate
DX109	18.5	18.6	21.6	Not detected
DX111	18.2	16.8	22.5	Not detected
DX114	18.1	15.1	22.0	19.2

* mean estimated based on two of three test replicates for the sample, whereas one of three replicates failed for IPC with invalid mLN34 detection results

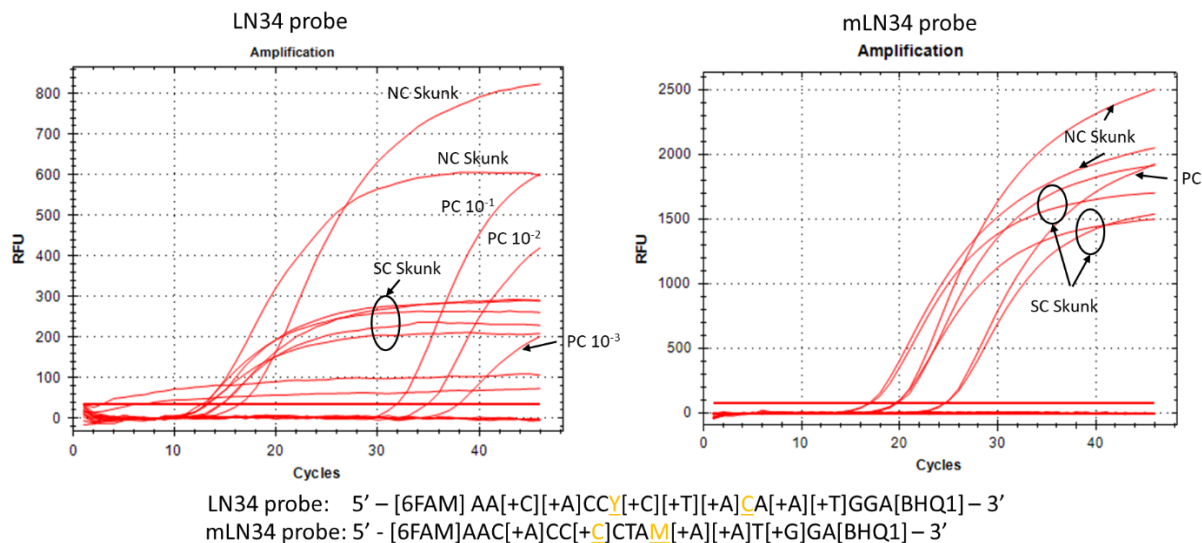
S5 Table. The mean cycle threshold values (C_i) across real-time reverse transcriptase PCR triplicate runs for the detection of a beta-actin internal positive control (IPC) and *Lyssavirus rabies* RNA (mLN34) in sublingual and parotid salivary gland (SG) tissues of skunks naturally infected with big brown bat (*Eptesicus fuscus*) variant (Ef-W1) in Coconino County during 2021-2023.

Laboratory ID	Sublingual SG		Parotid SG	
	beta-actin mean (IPC)	mLN34 result	beta-actin mean (IPC)	mLN34 result
AZ002	31.4	31.5	33.4	Not detected
AZ004	26.3	29.0	20.6	Not detected
AZ006	29.5	28.5	22.4	Indeterminate
AZ007	No tissue	Not tested	33.0	Indeterminate
AZ008	No tissue	Not tested	29.5	30.2
AZ011	33.2	37.5	24.2	Indeterminate
AZ012	30.3	33.7	23.6	Not detected
AZ013	Not detected	Indeterminate	24.6	Not detected
AZ014	33.2	Not detected	24.9	Not detected
AZ015	29.2	32.2	23.0	23.8
AZ017	32.4*	34.5*	28.2	Not detected

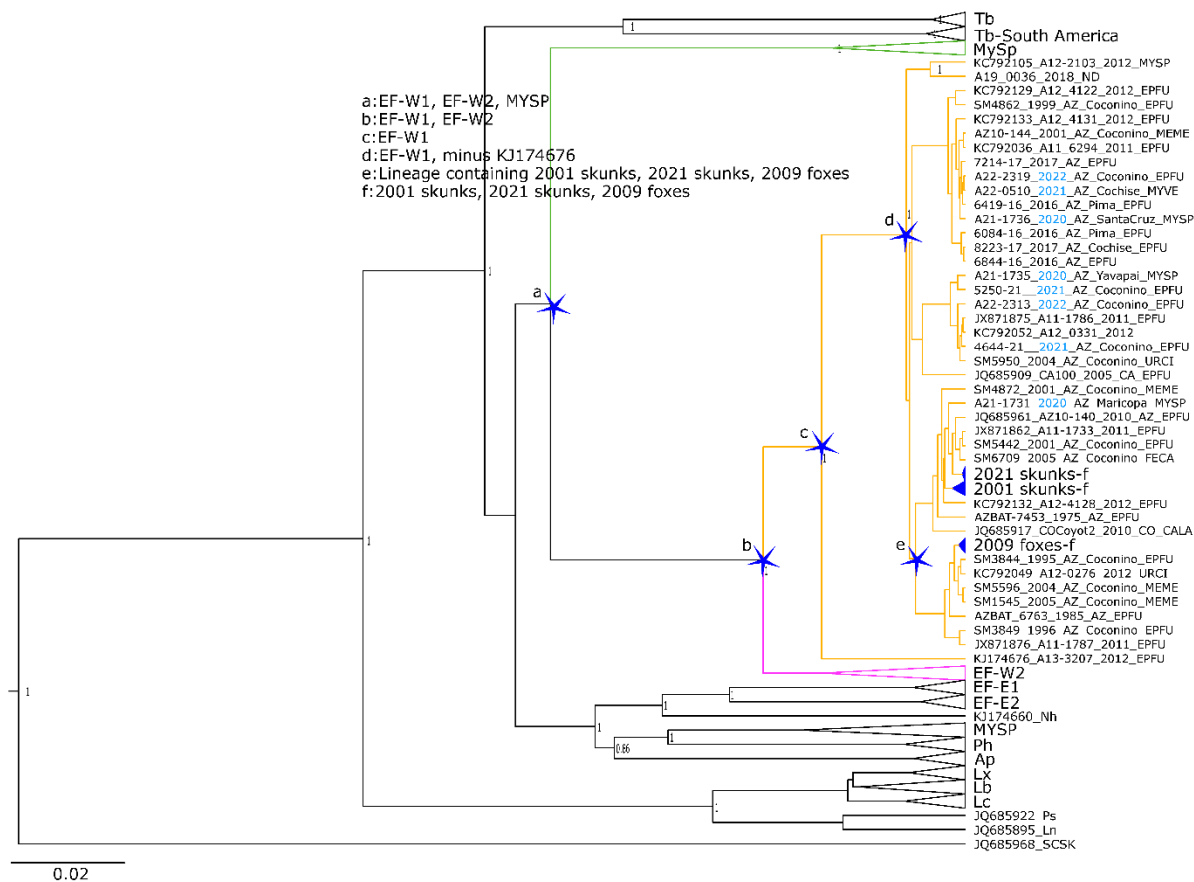
AZ018	33.4	Not detected	32.6	Not detected
AZ019	34.9	Not detected	31.1 [§]	31.6 [§]
AZ022	31.8	28.5	29.4	28.0
AZ023	33.2	33.1	30.3	30.0

* mean estimated based on two of three test replicates for the sample, whereas one of three replicates failed for IPC with invalid mLN34 detection results

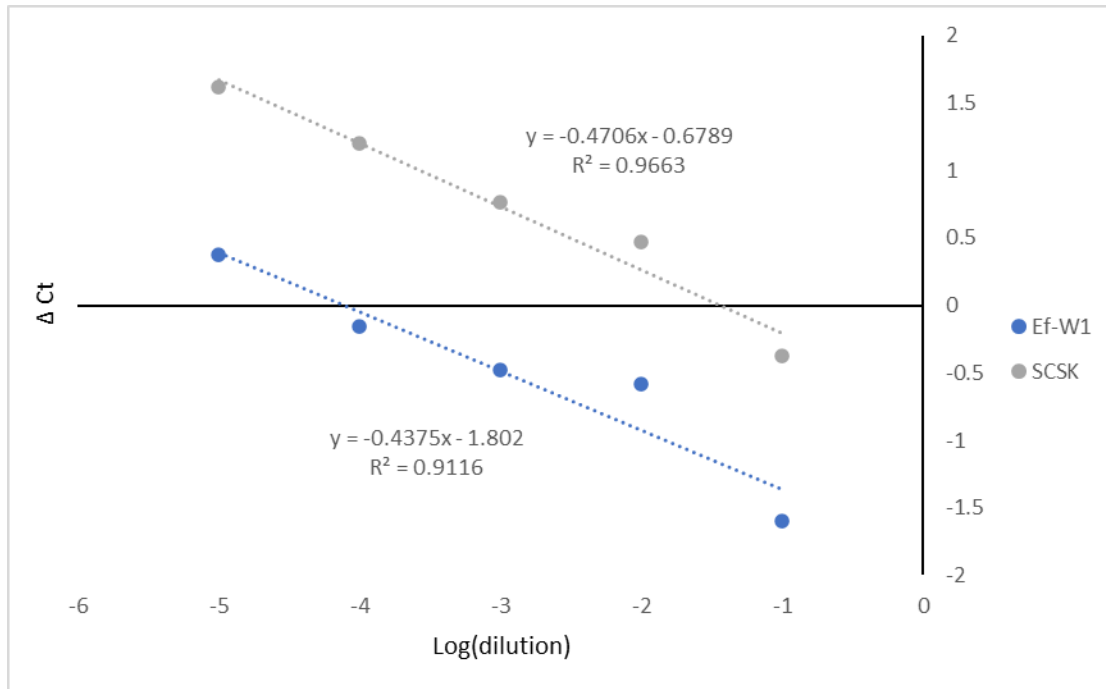
[§] mean estimated based on two of three test replicates for the sample, whereas one of three replicates had atypical curves and indeterminate mLN34 detection results



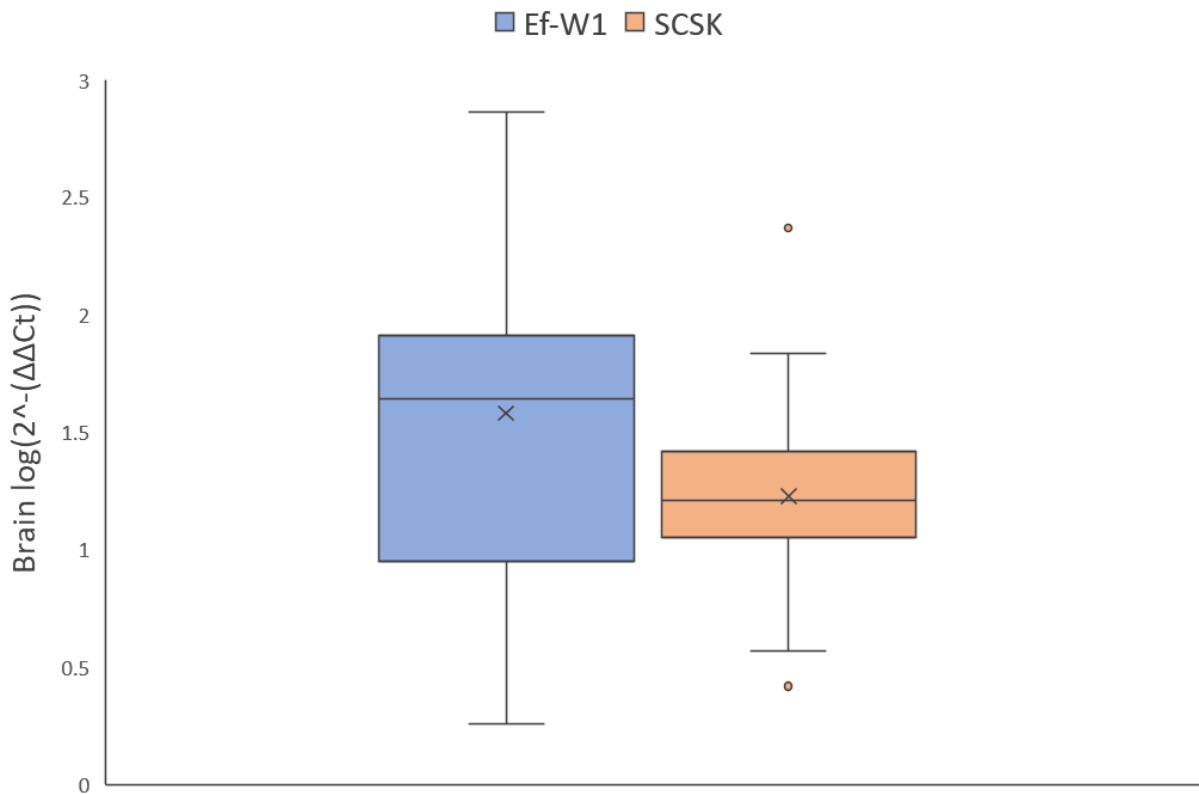
S1 Fig. Plots of the real-time reverse transcriptase PCR (rtRT-PCR) results and sequences comparing the reference LN34 probe and the probe mLN34 modified for the current study. [+N] represents locked nucleotides. We initially compared amplification of three *Lyssavirus rabies* (RV) variants, North Central skunk (NC skunk), South Central skunk (SC skunk), and a dog variant street virus as a positive control (PC). We modified the probe due to PCR inhibition when amplifying the SC RV skunk variant (left panel). Moving the location of ambiguous bases (highlighted in the sequences) and adjusting locked nucleotides resulted in similar levels of amplification for the mLN34 probe among the RV variants tested (right panel).



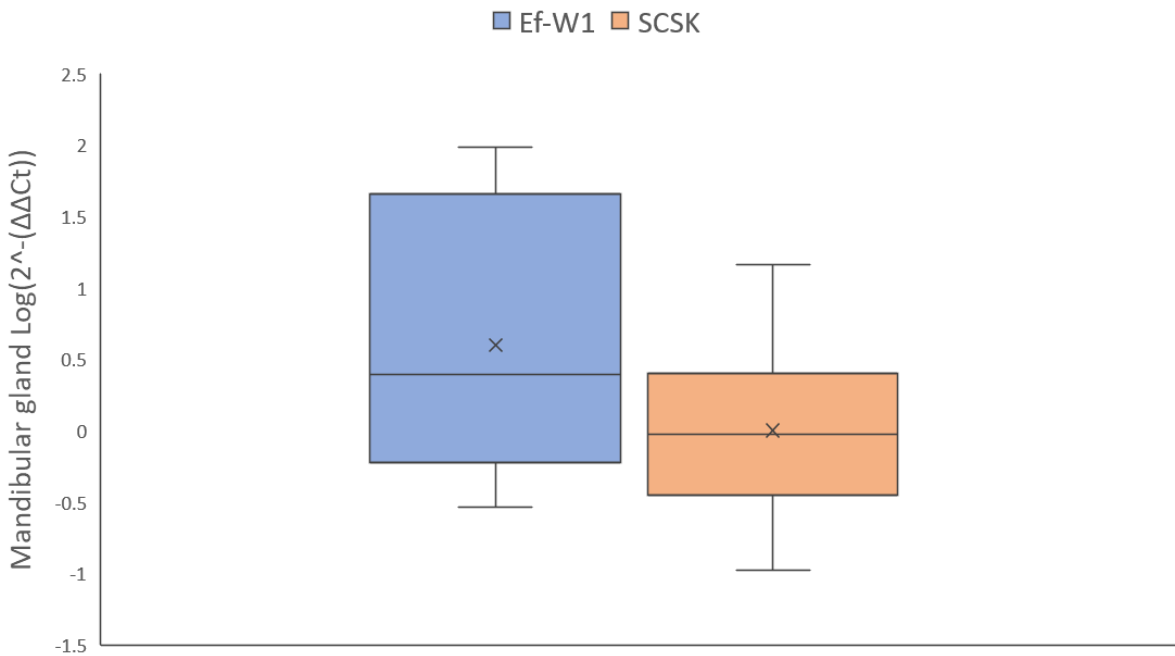
S2 Fig. Phylogenetic tree used in dN/dS analysis. Branches indicated in the legend and by letters and blue stars or triangles were tested independently for evidence of codons under positive selection relative to the rest of the tree. Several branches are collapsed for ease of viewing. Numbers on branch points indicate posterior support value. The *Lyssavirus rabies* (RV) variants are indicated by abbreviated names of the hosts they are associated with: Tb *Tadarida brasiliensis*, MySp *Myotis* sp, EF *Eptesicus fuscus*, Lx *Lasiurus xanthinus*, Lb *Lasiurus borealis*, Lc *Lasiurus cinereus*, Ph *Parastrellus Hesperus*, Ap *Antrozous pallidus*, Nh *Nycticeius humeralis*, Ps *Perimyotis subflavus*, Ln *Lasionycteris noctivagans*, and South-Central skunk (SCSK). Ef-W1, Ef-W1 and MySp RV variants are highlighted by yellow, pink, and green branches, respectively. Naming for Ef-W1 sequences is the same as Figs 3 and 4. Scale is in substitutions per site.



S3 Fig. Plot of ΔC_t values obtained against the RNA dilution series for two samples infected with *Lyssavirus rabies* (RV), for the big brown bat (Ef-W1) and South-Central skunk (SCSK) RV variants. From Livak and Schmittgen (2001), the slopes of the linear function should be similar to permit valid comparisons of ΔC_t values between samples or treatment groups and evidence of similar slopes for the two samples representing the RV variants compared in this study is shown.



S4 Fig. The difference between log transformed means of Ct values from real time reverse transcriptase PCR analysis to detect and quantify *Lyssavirus rabies* (RV) from brain tissues of skunks naturally infected with the Ef-W1 bat or South-Central skunk (SCSK) RV variants.



S5 Fig. The difference between log transformed means of Ct values from real time reverse transcriptase PCR analysis to detect and quantify *Lyssavirus rabies* (RV) from mandibular salivary gland tissues of skunks naturally infected with the Ef-W1 bat or South-Central skunk (SCSK) RV variants.